University of Stavanger

Faculty of Science and Technology

MASTER'S THESIS

Study program/ Specialization: **Offshore Technology/ Subsea Technology**	**Spring semester, 2012** **Open / ~~Restricted access~~**
Writer: **Kourosh Mashayekh**	(Writer's signature)

Faculty supervisor:

Ljiljana Djapic Oosterkamp (University of Stavanger, Stavanger, Norway)

External supervisor(s):

Anthonie Oosterkamp (Polytec, Haugesund, Norway)

Ljiljana Djapic Oosterkamp (Statoil, Stavanger, Norway)

Title of thesis:

Prediction of Response and Damaged Length of a Subsea Pipeline after a Full Bore Rupture

Credits (ECTS): **30**

Key words: **Subsea pipeline, Full bore rupture, OLGA, Pull-over, Local buckling/collapse, Finite element analysis, ANSYS, Dragging anchor**	Pages: **iv + 59** + enclosure: **19** **Stavanger, 15th August 2012**

Acknowledgements

This thesis is performed in order to fulfil the requirements of Master of Science degree in the Offshore Technology Master's Degree program at the Department of Mechanical and Structural Engineering and Materials Science, Faculty of Science and Technology, University of Stavanger, Norway. The thesis work was carried out at Polytec, Haugesund, Norway. It began in January 2012 and finished in August in the same year.

First of all, I would like to use this opportunity to thank my main supervisor Ljiljana Djapic Oosterkamp for giving me the chance of performing this thesis under her supervision. I would also like to thank her for advising me and supporting me. In addition, I would like to thank my co-supervisor Anthonie Oosterkamp for guiding me to learn the OLGA software and also for his technical supports while performing the work for the thesis. I would also thank him for his friendly attitude towards me. It was my honour to working with them.

I would also like to thank Statoil (Stavanger, Norway) for providing me with accommodation in Haugesund as well as giving me the opportunity to learn ANSYS at EDR^{TM} MEDESO (Sandvika, Norwya).

Further, I would also like to thank Polytec (Haugesund, Norway) for providing me an office space, ability to use their computer software such as ANSYS and OLGA. Additionally, I would like to express my gratitude to the Polytec for its full support and as well its friendly atmosphere.

In addition, I would like to thank EDR^{TM} MEDESO (Sandvika, Norway) for guiding me in using ANSYS software for the thesis work.

My sincere appreciation goes to my family. To be where I am now and to be able to obtain the Master degree I utterly owe to them. I would like to thank them specially my parents for their interminable supports and their mental support. I would also like to thank my older brother for backing me up all my life. In addition, I would like to thank my younger brother for making me laugh with his funny deeds.

At the end, I would like to take this opportunity to thank my best friends Armin Narimanzadeh and Riad El-Wardani for their mental support. I would also like to thank them for being with me and the cool and unforgettable experience with them during the last years.

Stavanger, August 2012

Kourosh Mashayekh

Executive Summary

The combination of oil and gas reservoirs in sea areas with high shipping traffic brings some challenges for engineers. One of these challenges is related to subsea pipeline systems specially where water depth is classified as shallow or intermediate. Due to large number of vessels passing the area with shallow water depth, interaction between anchors of these vessels and the offshore pipeline can occur. If a dragging anchor hits and subsequently hooks the pipeline, the pipeline could be ruptured. When an offshore pipeline ruptures while it is in operational mode, the operation must be stopped immediately and a repair team has to repair the pipeline system as quick as possible. On the key steps for repairing the pipeline is to remove and replace damaged length of the pipeline. Hence evaluation of the damage length is important. In this project, the response of a ruptured pipeline by an anchor load was studied to predict and define the damaged length.

In order to solve the problem, the solution method is split in three parts. In first step, the flow condition of hydrocarbons inside the pipeline as well the fluid interaction with the pipeline is calculated using one dimensional pipe flow software OLGA.

During the second step, the mechanical response of the pipeline to load applied by the caught anchor is determined. The reaction of the pipeline from the moment after impact until rupture is studied using finite element analysis. ANSYS Workbench 14 software is used in this step.

The third step determines the deformation of the subsea pipeline after rupture. A jet of released hydrocarbons will lead to a thrust force on the ruptured cross-section. This force causes the ruptured pipeline to buckle. Purpose of this part is to identify where local buckling occurs and whether the pipeline collapses due to buckling or not. If the pipeline fails at buckled region, pipe's sections from the buckled pipe's cross-section to ruptured pipe's cross-section have to be cut. This step is also done with finite element analysis using the ANSYS software.

In this project a pipe section with length of $3000\ m$ and outer diameter of $42''$ is modelled in ANSYS. Obtained results show that the displacement of the pipeline before rupture is already severe. According to the results, after rupture, the result is thrust force leads to either sides of the ruptured pipeline to buckle and fail at two regions. Hence, repair team has to cut the pipeline from the buckled pipe's cross-sections. The thrust force from the escaping fluid jet leads to additional length of pipe to be cut.

Table of Contents

List of Figures

List of Tables

List of Abbreviations and Symbols

Abbreviations

APDL	ANSYS Parametric Design Language
DNV	Det Norske Veritas
LC condition	Load Controlled condition
DC condition	Displacement Controlled condition
3-D	Three Dimensional
Max.	Maximum
Min.	Minimum
W.T	Wall Thickness
Sys	System
CV	Control volume

Latin Symbols

A	Area of cross-section
A_s	Contact surface area
C_L	Lift coefficient
C_P	Specific heat capacity
$d\vec{F}$	Net force
dF_{Bx}	Body force in *X*-direction
dF_{Sx}	Surface forces in *X*-direction
dF_x	Net force in *X*-direction
dm	Mass of an infinitesimal system
d_s	Element area
D	Diameter
D_i	Inner diameter
D_{out}	Outer diameter
e	Elongation
E	Modules of elasticity
E_n	Total stored energy
f	Darcy-Weisbach friction factor
f_o	Out of roughness
f_{cb}	Minimum of f_y and $\frac{f_u}{1{,}15}$
f_y	Yield stress to be used in design
$f_{y.temp}$	De-rating on yield stress to be used in design
f_u	Tensile stress to be used in design
$f_{u.temp}$	De-rating on tensile stress to be used in design
F	Pushing force
F_B	Buoyancy force
F_C	Coulomb friction load
F_L	Vertical (lift) force
F_R	Passive resistance
F_s	Resisting force of spring
g	Acceleration of gravity
h	Convection heat transfer coefficient
h_1	Heat transfer coefficient of fluid
h_2	Heat transfer coefficient of sea water
H	Height difference
K	Conductivity of pipe

K_s	Is a constant defined as: $\frac{\gamma_s{}' \cdot D^2}{N - F_L}$
K_{sp}	Stiffness of spring
L	Length
$L_{initial}$	Initial length
L_{new}	New length
m	Mass
$\dot{m}$	Mass flux
$\dot{m}_0$	Mass flux at t_o
$\dot{m}_1$	Mass flux at t_1
$m_{abso.\ w.}$	Mass of absorbed water
$m_{anti-corr.}$	Mass of anti-corrosion layer
$m_{concrete}$	Mass of concrete layer
$m_{contents}$	Mass of contents
m_{steel}	Mass of steel per meter
m_{total}	Total mass of pipeline
M_u	Molar mass of gas
n	Number of moles (mass)
N	Submerged weight
N_u	Nusselt number
P	Pressure
$\bar{P}$	Average pressure
P_0	Pressure at t_0
P_1	Pressure at t_1
$P_b(t)$	Pressure containment resistance
$P_{end\ point}$	Pressure at last point
P_i	Internal pressure
P_{min}	Minimum internal pressure
P_r	Prandtl number
$P_{start\ point}$	Pressure at beginning point
P_T	Tensile load
P_o	Outside pressure
$\dot{Q}_{cond,cyl}$	Conduction heat transfer rate of a cylindrical tube
$\dot{Q}_{conv}$	Convection heat transfer rate
$\dot{Q}_{net_{in}}$	Net rate of heat transfer into a system
$\dot{Q}_{tot}$	Total heat transfer
r_1	Inner radios
r_2	Outer radios
R	Gas constant
R_e	Reynolds number
R_{tot}	Total modelled heat resistance
R_u	Molar gas constant
t	Wall thickness
t_o	Rupture moment
t_1	Next step after rupture
t_{corr}	Corrosion allowance
t_{fab}	Fabrication roundness
T	Temperature
$\bar{T}$	Average temperature
T_0	Temperature at t_0
T_1	Temperature of inner surface
$T_{1\infty}$	Temperature of fluid
T_2	Temperature of outer surface
$T_{2\infty}$	Ambient temperature
T_e	Temperature at beginning section
T_i	Temperature at ruptured point
u	Velocity in *X*-direction

u'	Velocity of fluid through an elemental area
$\bar{u}$	Average velocity
u_0	Velocity at t_o
u_1	Velocity at t_1
v	Velocity in *Y*-direction
V	Total velocity
$\vec{V}$	Field velocity
V_c	Current velocity
V_o	Volume
$V_{o_{system}}$	Volume of system
$V_{submerged}$	Displaced volume of water
w	Velocity in *z*-direction
W	Weight in air
$\dot{W}_{net_{in}}$	Net rate of work transfer into a system
X	Initial location in *X*-direction
X'	Final Location before rupture in *X*-direction
X''	Final Location before rupture in *X*-direction
X_s	Elongation of spring
Y	Initial location in *Y*-direction
Y'	Final Location before rupture in *Y*-direction
Y''	Final Location before rupture in *Y*-direction
Z	Compressibility factor
Z_P	Penetration depth

Greek Symbols

α	Coefficient of thermal expansion
α_{gw}	Girth weld factor
α_h	Minimum strain hardening
α_u	Material strength
γ_ε	Strain resistance factor
$\gamma_S{}'$	Submerged unit soil
Δm	Deference of mass
ΔT	Temperature difference
ΔP	Pressure drop
ε	Strain
ε_e	Elastic Strain
ε_P	Permanent strain
ε_{Rd}	Design resistance strain
ε_{Sd}	Design compressive strain
ε_T	True strain
ϑ	Poisson's ratio
μ	Dynamic viscosity
μ_f	Coefficient of friction
ρ	Density of fluid
$\dot{\rho}$	Density rate
$\bar{\rho}$	Average density of fluid
ρ_0	Density at t_0
ρ_1	Density at t_1
$\rho_{anti-corr.}$	Density of anti-corrosion
$\rho_{concrete}$	Density of concrete
$\rho_{contents}$	Density of contents
$\rho_{(t)}$	Density function
ρ_{steel}	Density of steel
ρ_{water}	Density of water
σ	Normal stress
σ_{xx}	Normal stress in *X*-direction

σ_U	Ultimate stress	τ_{yx}	Shear stress in *Y*-direction
σ_Y	Yield stress	τ_{zx}	Shear stress in *Z*-direction
τ_{ij}	Shear stress		

1 Introduction

Having seafood resources as well as hydrocarbon resources has made the oceans an important part of man's existence. Thus, humans always attempt to utilize the available resources as much as possible in order to increase the quality of live. Invention of ships and subsequent improvements of the shipbuilding industry were the main drivers towards increased usage of the sea. Nowadays, massive fishing ships and huge trading vessels move on the sea surface in order to fish and transport various goods from place to place.

Besides this mentioned usage of sea, different technologies have been implemented to extract the hydrocarbons from offshore reservoirs. Therefore, massive tankers or submarine pipelines are used in order to transport the hydrocarbons from offshore reservoirs to desired onshore terminals or to another offshore platform. Depending on the conditions sometimes a submarine pipeline system is a better solution compared to a tanker. The subsea pipeline system has its own challenges. One of the noteworthy challenges is the interaction between fishing gear, dragging anchors or dropped objects and offshore pipelines. The consequence of these types of incidents could be very serious and must therefore be considered.

Various problems can occur in realm of offshore pipeline systems; thus before beginning the project, one should describe the types of problems that could be made if an incident happens as well as consequences.

1.1 Problem Statement

The main consequences of a damaged submarine pipeline are fire, explosion, injury, loss of life, environment pollution, loss buoyancy around a vessel, economic loss, decreasing of follow capacity and increasing the difficulty of maintenance (HSE, 2009).

Generally two accidental loading scenarios are considered when the discussion is about serious damage of a riser or a pipeline. First case is impact loading (mostly due to dropped object) and the second scenario is pull-over/hooking (mainly due to a dragged anchor or a trawl board) (DNV, 2010b).

In this project the pull-over/hooking case is studied. Interaction between an anchor and a submarine pipeline has various reasons. It can occur by a ship dragging an anchor (due to improper deployed anchor or intense weather conditions), an emergency anchoring which might be due to anchoring related to offshore activities or engine failure. Consequences of the incident are listed below:

- Destroy the pipeline protection, for example the rock cover that weakens the pipeline with respect to future threats.
- Applied impact load from the anchor can destroy the coating layers. If the coating layers are damaged, it will increase requirements for cathodic protection .In addition, the impact load can cause dents inside the pipe. Dents reduce flow capacity or even block the pipe as well as increasing the difficulty of internal inspection or maintenance. It should be noticed in some cases, the pipeline is breached and the contents might be released. If the contents is gas,

bubbles will go up to the surface which can make buoyancy of the vessel unstable, increase the risk of asphyxiation of crews as well as the risk of explosion.

- If the anchor hooks the pipeline and pulls the pipe, more dents will be induced due to the pullover. It should be noticed that the dents decrease the pipeline fatigue life under operational conditions.
- Large displacement of the pipeline can occur due to pullover of the pipe. This large displacement cause buckling or rupturing the pipeline. In the case of rupture compared to other mentioned cases, a longer part of pipeline will be damaged and the amount of released hydrocarbons will be more substantial. The consequences will also be more severe (HSE, 2009).

In this study it is assumed that the anchor pulls the pipeline and finally the pipe is ruptured due to pullover. The accident leads to releasing a hydrocarbon jet in the water. In order to reduce the consequences, production has to be stopped immediately and required repair action must be done. This type of incident can be studied from various aspects; thus a specified intention of the mentioned case must be defined.

1.2 Scope and Objectives

As it was mentioned, the project focuses on a subsea pipeline that is hooked by a dragging anchor. The anchor pulls the pipeline and finally it ruptures the submarine pipeline. Damaged section must be removed and replaced in order to repair the submarine pipeline system. Since these types of incidents cause serious problems such as environmental pollution and economical loss, the repair team must reduce the downtime as much as possible. One of the items for decreasing the downtime and repairing the transport system is knowing the pipe's damaged length prior to an incident. Storing the needed pipe's sections makes the repair team ready to act and increase the efficiency of the repairing process. Thus, this project rationale is to predict the pipeline's damaged length with respect to described scenario.

1.3 Limitations

The project is endowed with the below limitations. In order to eliminate the limitations and continue to survey the case, some assumptions have been made which are explained further.

- Unknown imperfectness of steel pipeline, anti-corrosion coating and concrete coating
- Complexity of three dimensional motion of the pipeline before and post rupture
- Complexity of determining shape of ruptured pipeline's cross-section
- Complexity of considering effects of butt weld between pipe sections
- Reduction of the ultimate strength of steel due to corrosion defects
- Complexity of the interaction between seabed and the pipeline

1.4 Methodology

To obtain the required information about the project, related papers, books and published standards have been studied. The papers were mostly recommended by the faculty supervisor while the

standards were downloaded from the internet which related websites as well as other references will be mentioned in the *References*.

Three books were used; one of them (Introduction to Fluid of Mechanics) was studied in bachelor program and the others (Physical Fluid Dynamic and Advanced Mechanics of Materials) were used in the master program.

In addition to learn ANSYS software, a three days course organised by EDR^{TM} MEDESO (Sandvika, Norway) was useful while the OLGA software was learned with help of the external supervisor. It should be mentioned that having meetings with experienced engineers organised by faculty supervisor were very helpful to increase the comprehension of the problem.

2 Structure of the Report

This chapter breaks down and presents the structure of this report.

The first chapter, *Key Assumptions*, represents basic assumptions related to seabed, pipeline route, operational conditions, used material for the pipeline as well as the hydrocarbon compositions.

The next chapter, *Case Study*, provides a complete description of the problem and presents the scenario, challenges, limitations and related assumptions. This allows the reader to visualize the problem through its different stages.

Next, the *Theory* is addressed, which identifies the basis of analysis that is inherent in the modelling software packages used. In addition, the *Theory* chapter highlights the practical assumptions and limitations of the underlying theory. In an attempt to breakdown the problem and simplify its resolution, the theory is broken down into three main parts that are followed throughout the report. First part is related to *Fluid Mechanics* theory and describes the fluid flow characteristics of the carried hydrocarbons; it is important to consider this behaviour since it provides important insight into where along the pipeline the maximum flow rate occurs. This will cause the most severe incident, in the case of a rupture. Secondly, stress-strain theory is presented, which describes the pipeline behaviour during the initial stage of the scenario, when the anchor strikes and pulls a section of the pipeline beyond its plastic limit and up to rupture. Post-rupture characterizes the third part, which then relies on buckling theory to describe the behaviour of the pipeline.

Once the underlying theory is described, the *Analyses and Results* chapter presents the three models, each simulating the behaviour of one part of the scenario as described in the *Theory* chapter. The first model presented within this chapter is created in OLGA software and simulates the fluid flow parameters within the pipeline. Along with the model itself, assumptions and results are presented, which are required for the subsequent models. Based on the location of maximum flow rate obtained from this model, a combination of load scenarios are applied to the pipeline to find the lowest load combination that will cause it to bend beyond its ultimate strength. This is achieved by applying the stress-strain theory and simulating the behaviour in ANSYS, which is presented as the second model within the *Results and Analysis* chapter. The third and final model presented in this chapter is the buckling model, also carried out in ANSYS, which simulates the post-rupture behaviour of the pipeline and provides the results for the solution of the original problem of this project that is to define the minimum cut-length of damaged pipe during pipeline repair operations.

Finally, before summarizing the findings of the project, the results obtained by the above mentioned programs will be analysed to compute the total damaged length of the pipeline.

In the *Discussion*, the result and final answer are discussed to identify the reliability of the solution. The *Discussion* is based on the assumptions, limitations and results of the models in providing the solution to the original project problem.

To complement the findings of the project, the *Challenges* chapter includes the specific trials and challenges faced during the accomplishment of this work over the past months. It demonstrates that

although there were several hurdles along the path towards the solution, these were resolved to be able to achieve the overall objectives of the project.

Recommended *Areas of Further Work* is suggested to enhance the findings and further develop the models before turning to the *Conclusion* which captures and summarizes all the parts of this report.

3 Key Assumptions

This project predicts response of a submarine pipeline after a full bore rupture, thus it is necessary to generate some assumptions related to pipeline route, seabed features, hydrocarbon compositions and properties of used materials. The initial assumptions are listed below.

3.1 Seabed features

The seabed is assumed to be perfectly flat covered by soil with submerged unit soil (γ_S') around $12100\,{}^{N}/_{m^3}$.

3.2 Materials

In order to analyse the pipeline route with high accuracy, not only it is necessary to know properties of used materials to fabricate the pipeline, but also the features of fluid inside the pipeline and environment characteristics must be considered. The related assumptions are mentioned below.

3.3 Design life

The pipeline route has been designed with 50 years of lifetime.

3.4 Operational Data

Two different design pressures have been used in the analysis of the pipeline system:

$250\ bar$

$215\ bar$

It should be noticed that the incident pressure is $1.05 \times Design\ pressure$ and also the Test pressure is equal to $1.05\ \times\ 1.05\ \times Design\ pressure$.

The other engineering information that is needed is mentioned below.

Transport Medium	: Dry natural gas
Service Condition	: Sweet service
Maximum Hydraulic Capacity	: $84\ mill\ {}^{Sm^3}/_{d}$
Maximum Design Temperature	: $+50$ ℃ $(inlet)$
Minimum Design Temperature	: -10 ℃

3.5 Hydrocarbon Compositions

The investigated fluid is dry gas with a composition of N_2, CO_2, $C1$, $C2$, $C3$, $IC4$, $NC4$, $IC5$, $NC5$ and $C6+$. Assumed composition of the gas is represented by *Table 1*.

Table 1. Pipeline Gas Composition

	Composition	
	Mole (%)	Mole weight
N_2	0.3553	
CO_2	0.2648	
C1	93.8364	
C2	3.4738	
C3	1.2750	
IC4	0.2217	
NC4	0.2947	
IC5	0.0927	
NC5	0.0864	
C6+	0.0978	90.99
H_2O	0.0013	
Total	100	17.5

3.6 Material Mechanical Data of Pipeline

In order to survey the pipeline, it is recommended to consider a steel grade that is used a lot in oil and gas industry. Thus *SWAL 450 I DF (X65)* is chosen. More details of steel *X54* are mentioned by *Table 2*.

Table 2. Pipeline Design Conditions

Steel Designation		X65
Specified Min. Yield Strength		450 MPa
Specified Min. Tensile Strength		535 MPa
Density	ρ_{steel}	7850 kg/m^3
Modulus of Elasticity	E	207 GPa
Poisson's Ratio	ϑ	0.3
Coefficient of Linear Thermal Expansion	α	$1.16 \cdot 10^{-5}$ °C^{-1}
Specific Heat Capacity	C_P	0.5 kJ/(kg·k)
Thermal Conductivity	K	50 W/(m·k)

3.7 Line Pipe Diameters

Pipe with outside diameter 42'' has been selected by the designer and the more data related to designed pipe are listed in *Table 3*.

Table 3. Detail of the designed pipe

Pipeline Nominal Outside Diameter		D_o	42''
Pipeline Inside Diameter (Constant)		D_i	1016 mm
Incident/Design Pressure Ratio			1.05
Out of Roundness		f_o	1.5% D
Corrosion Allowance		t_{corr}	0 mm
Fabrication Tolerances		t_{fab}	±1.0 mm
Safety Class (DNV, 2010a)	Operating		Normal (zone 1) & High (zone 2)
	System Test		Low
	As-Laid		Low
	Installation		Low

3.8 Internal and External Coatings

It is assumed that one layer is used to create the internal coating while two different layers (*Anticorrosion* and *Concrete*) are utilized in order to cover the external side of the pipe. More assumed properties of selected internal and external coatings are presented hereinafter:

3.8.1 Internal Coating

Type of coating	: Liquid Epoxy
Typical coating thickness	: $60 - 80\ microns$
Typical coating density	: $1500\ kg/m3$

3.8.2 External Coating

External coating consists anticorrosion and concrete.

Anticorrosion

Type	: Fiberglass reinforced asphalt enamel
Wall thickness	: $6\ mm$
Density	: $1300\ kg/m3$

Concrete

Concrete Density	: $2250\ kg/m3$
Concrete Coating Water Absorption	: Min. 2% , Max. 4% by weight
Concrete Coating cut-back	: $390\ mm\ \pm\ 10\ mm$

3.9 Pipeline Route

In this project, it is assumed that the pipeline is located in The North Sea with a length close to $626\ km$. In order to have an accurate analysis, it is split into 24 sections with different lengths and elevations. Additionally, various steel and concrete wall thicknesses are assumed. *Table 4* represents more details of the pipeline sections.

Table 4. Lengths, Elevations and Wall thickness of the Pipe Sections

Pipeline Section		Depth at Starting Point (m)	Depth at Ending Point (m)	Length (Km)	Steel W.T (mm)	Concrete W.T (mm)
From	To					
KP000	KP010	-186.4	-235	10	34.1	65
KP010	KP020	-235	-270	10	34.1	65
KP020	KP025	-270	-175	5	34.1	65
KP025	KP040	-175	-175	15	34.1	65
KP040	KP060	-175	-75	20	34.1	45
KP060	KP070	-75	-160	10	34.1	45
KP070	KP090	-160	-95	20	34.1	45
KP090	KP140	-95	-215	50	34.1	45
KP140	KP160	-215	-140	20	33.3	45
KP160	KP185	-140	-235	25	33.3	45
KP185	KP190	-235	-200	5	33.3	45
KP190	KP195	-200	-160	5	33.3	45
KP195	KP210	-160	-220	15	33.3	45
KP210	KP225	-220	-240	15	33.3	45
KP225	KP250	-240	-340	25	33.3	45
KP250	KP260	-340	-355	10	33.3	45
KP260	KP300	-355	-370	40	33.3	45
KP300	KP340	-370	-335	40	33.3	45
KP340	KP370	-335	-130	30	33.3	55
KP370	KP375	-130	-120	5	29.1	70
KP375	KP400	-120	-110	25	29.1	70
KP400	KP600	-110	-110	200	29.1	70
KP600	KP626	-110	-82	25.98	29.1	70
KP626	KPEND	-82	0	0.32	33.3	50

4 Case Study

This chapter provides a comprehensive description of the problem, assumptions and associated limitations of the model. It attempts to set the scene for the reader and establish a basis upon which a suitable theory may be applied to solve the problem stated in the *Problem Statement* section (*see chapter 1-section 1*).

Consider the offshore pipeline previously lying flat on the seabed within an area that is prone to shipping traffic with large vessels. Modern fishing equipment is a source of concern for such pipelines due to the intensive fishing gear used for supporting the nets. In this case, the unfortunate event of a collision between one of those large anchors and the pipeline is considered where the pipeline is relocated due to the large dragging forces. The anchor imposes an external point load on the pipeline, which in addition to displacing it, also bends it. Consequently, a maximum deflection will occur at the hooking point (centre). Once the pipeline starts to move, resisting forces due to friction between the pipeline and the seabed will restrict this displacement. The resisting forces are dependent on the dimensions of the pipeline as well as the penetration depth within the soil. Effectively, while the applied hooking load at the centre of the pipeline pulls the pipeline, along the pipeline it is countered by the resistance forces. Hence, effect of the hooking load is diminished by the resistance forces along the pipeline. Therefore, where the soil resistance is significant enough to totally eliminate the effect of the hooking load, the pipeline is stopped to move. At those points, where the pipeline does not move, it is considered as though there were fixed supports which induce axial loads on the pipeline section in between.

In this case study, it is assumed that not only does displacement occur and the pipeline bends, but also that the load is significant enough to rupture the pipe.

For simplicity purposes, it is assumed that the section of pipe between the two virtual fixed anchor points is of a constant length. In practical sense, the length of the section is increased slightly due to the displacement and bending while the axial loads also increase. Finally, the axial loads become larger than the ultimate strength of the pipe material and the pipeline ruptures.

Figure 1 has been drawn to illustrate the case to the reader. *Figure 1a)* shows the moment of incident between the anchor and the pipeline while *Figure 1b)* illustrates how the pipeline bends due to the anchor force. The anchor load, axial forces, resistance forces and the fixed supports are illustrated by black, blue, red and green colours, respectively.

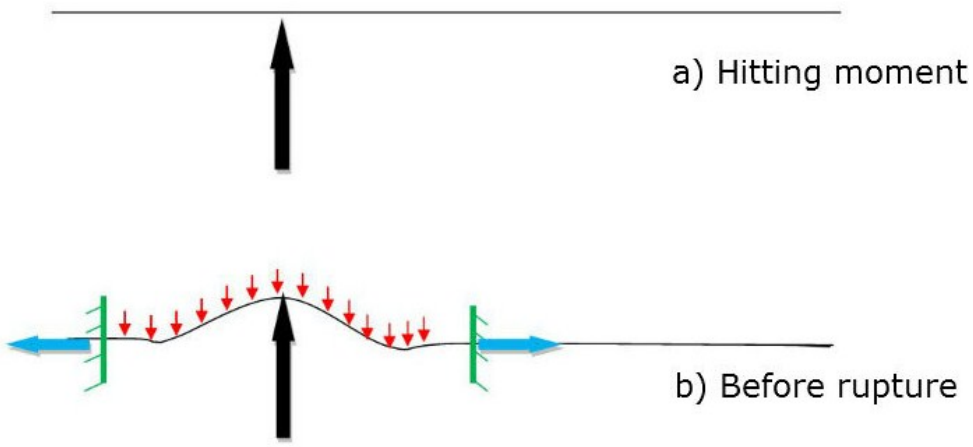

Figure 1. Movement of the Pipeline

Once rupture occurs, the hooking force is removed and transported process fluid will emit as a hush pressure jet out of the pipeline. It is assumed that upon rupturing, the pipeline maintains its circular cross-section, i.e. a clean cut. Fluid flow out of the ruptured end creates a reactive force perpendicular to the cross-section of the pipeline, which pushes the pipeline back towards the fixed anchor points described above. This leads to buckling of the pipeline near the ruptured end due to the special shape of the pipeline section just after rupture. Response of the pipeline to this reactive force depends on the magnitude of the force, length of the pipeline section, initial deflection prior to rupture and the features of the seabed.

Subsequent to rupture, boundary conditions change and a symmetrical problem is considered where only one side of the pipeline is analysed. Fluid properties, such as density and flow rate, must be determined since they will affect the loads on the pipeline after rupturing. Only the section with maximum flow rate along the length of the pipeline is considered, since this will result in the largest forces due to the proportional relationship between the flow rate out of the ruptured pipeline end and the resultant jet force.

Figure 2 shows the boundary conditions and the pipeline condition just after the rupture moment. Similar to *Figure 1*, the resistance force and the fixed support are illustrated by red and green colour respectively, while the force made by the fluid flow out is shown by blue colour.

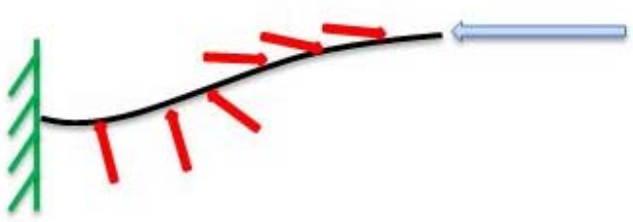

Figure 2. Condition of the Pipeline after the Rupture

5 Theory

According to the generated Key Assumptions and Case Study, in order to choose a proper solution the underlying theory was studied. The theory is expressed thoroughly in this chapter in more details in this chapter.

The solution is made in three main parts:

- Fluid's flow conditions during the incident. This part is subdivided into two sections. Before the rupture, the flow is considered as a steady state flow. The steady state must be calculated as it affects the post rupture condition of the pipeline as well as the thermal stresses induced due to the temperature difference of the fluid and the seawater. The second part referring to the post rupture is transient flow. Intention of investigating post-rupture flow is to determine the worst case scenario concerning the rupture location, as well as the magnitude of the force applied by the escaping fluid jet from the broken pipe's cross-section after rupture. These parts are linked, and are treated together.
- The pipeline reaction to the anchor load. One must define the effects of the load to the pipeline from the impact moment until rupturing. This stage of the studies defines the deflection of the pipeline and the shape of the pipeline just before the rupture. The configuration of the pipeline before rupture influences the pipe's response to the post rupture's condition.
- Response of the pipeline to the applied force by the escaping fluid jet. This section defines the damaged length of the pipe, i.e. the length of pipe that must be cut and replaced.

To comprehend the adopted solution for this project, it is necessary to have the knowledge related to fluid mechanics and heat transfer as well as mechanics of material. For estimating the mass flow rate, density of the fluid after the rupture and the resulting force that the fluid jet applies on the cross-section of the pipeline, selected concepts of fluid mechanics and heat transfer are needed, while the knowledge of mechanics of materials will be needed to analyse the response of the pipeline to different loads.

5.1 Fluid Mechanics and Heat Transfer

Concepts of fluid mechanics are required to simulate the fluid flow behaviour inside the pipeline and its effect on the pipeline. It is used to identify the flow rate and pressure within the pipeline before rupture as well as various parameters after rupture. Such parameters include leakage rate and change in density, pressure and temperature of the fluid with respect to time, after rupture has occurred.

5.1.1 Steady and Unsteady State Flow

If the imposed conditions of a flow do not change over time, the flow is called steady state (Tritton, 1998). The flow before the rupture is assumed to be steady state flow thus the fluid's properties will not alter with time.

$$\frac{\partial}{\partial t} = 0 \qquad (1)$$

The unsteady state flow which is known also as transient flow occurs when the conditions are not constant over time.

5.1.2 Mass Conservation Law

In relation to fluid flow through the pipeline prior to rupture, the mass conservation law implies that matter cannot be lost or created within a closed system; i.e. mass must be conserved. The concept is that the mass in the control volume can neither be created nor destroyed, thus the mass of the fluid in the pipeline can be estimated. This physically translates into that the mass introduced into the closed system, the pipeline in this case, at the inlet point must be contained within the closed system, with no losses or gains over time. The mathematical representation of the law for a system with mass, *m*, can be written as (Fox, 2004):

$$\left.\frac{dm}{dt}\right|_{Sys} = 0 \tag{2}$$

where *m*, based on the relation *mass = density x volume*, can be represented as :

$$m_{system} = \int_{Sys} dm = \int_{V_{o_{Sys}}} \rho dV_o \tag{3}$$

where $V_{o_{sys}}$ is the volume of the system and ρ is the density of the fluid.

Furthermore, the continuity equation presented below is developed using the mass conservation law as a basis.

5.1.3 Continuity Equation

Continuity equation, as shown in *Figure 3*, expresses the mathematical relation stating that mass flow rate into a control volume, is equal to the combination of mass flow rate out of that control volume, plus the rate of change of mass within the control volume.

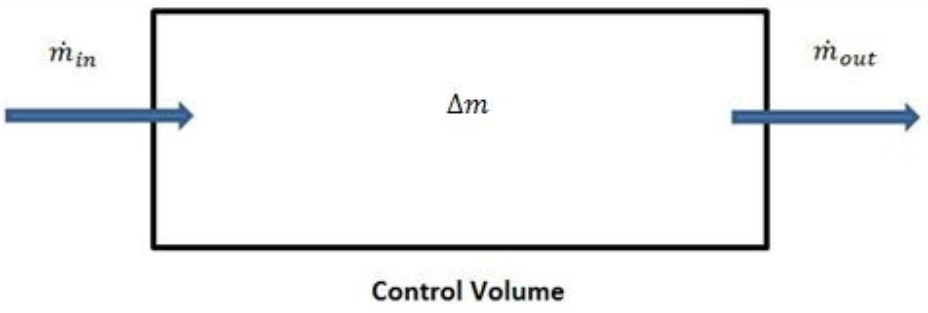

Figure 3. Concept of Continuity Equation

Consider a control volume as presented in *Figure 4* where fluid flows into or out of the volume across two parallel faces, as shown.

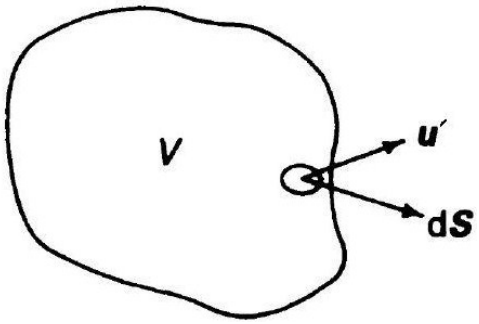

Figure 4. Definition Sketch for Derivation of Continuity Equation

An elemental area of *dS* is chosen within the control volume where the velocity of fluid flowing through this area is designated *u'*. According to Tritton (1988), the mass flow rate through the entire control volume can be described as a summation of such elemental areas throughout the control volume, as shown below:

$$\dot{m}|_{CV} = -\int_{CS} \rho u' \cdot dS \tag{4}$$

The negative sign appears, due to the assumption that the mass inside the control volume is increasing.

From definition of mass it can be written:

$$m = \int_{CV} \rho dV_o \Rightarrow \dot{m} = \frac{d}{dt}\int_{CV} \rho \, dV_o = \int_{CV} \frac{\partial \rho}{\partial t} dV_o \tag{5}$$

Continuous with equation (4):

$$\int_{CV} \frac{\partial \rho}{\partial t} dV_o = -\int_{CV} \rho u \cdot dS \tag{6}$$

As the aim is to define the mass balance at a point, the volume is very small. Thus the above equation is developed bellow:

$$\frac{\partial \rho}{\partial t} = -\lim_{V \to 0} \left[\int \rho u \cdot dS / V_o \right] \tag{7}$$

Which is:

$$\frac{\partial \rho}{\partial t} = -div\, \rho u \Rightarrow \frac{\partial \rho}{\partial t} + \nabla.(\rho u) = 0 \tag{8}$$

In the project the mass flow rate must be estimated and this equation helps to achieve the goal. According to the mass conservation law and this equation, by known mass flow rate upstream and the density rate through the pipe, the mass flow rate out of the pipe can be calculated.

5.1.4 Energy Equation

This equation is a statement of the first law of thermodynamic. The first law of thermodynamic states that increasing rate of the total stored energy of a system equals to the increasing rate of the net energy added to the system by heat transfer into the system plus the increasing rate of the net energy added to the system by work transfer into the system. The symbolic form of this equation is (Munson, 1998):

$$\frac{D}{Dt}\int_{Sys} E_n \rho \, dV_o = \left(\dot{Q}_{net_{in}} + \dot{W}_{net_{in}}\right)_{System} \tag{9}$$

Where:

E_n is the total stored energy of the system

$\dot{Q}_{net_{in}}$ is the net rate of heat transfer into the system

$\dot{W}_{net_{in}}$ is the net work transfer into the system

This equation is needed due to the heat and work transfer between fluid inside the pipeline and the seawater. More detail of heat and work transfer will be explained further.

5.1.5 Real Gas versus Ideal Gas

An ideal gas is a theoretical gas that obeys the below formula (Savidge, 2000):

$$\frac{PV_o}{nRT} = Z \tag{10}$$

Where:

P is pressure of the gas

V_o is volume of the gas

T is temperature of the gas

n is number of moles (mass)

Z is compressibility factor

For an ideal gas Z is 1 while for each real gas it is unique.

R is gas constant and it is defined by (Fox, 2004):

$$R = \frac{R_u}{M_u} \tag{11}$$

Where R_u is molar gas constant and M_u is molar mass of the gas.

Equation (10) is also shown by (Fox, 2004):

$$\rho = \frac{P}{RT} \tag{12}$$

Where ρ is density of the gas. Since Z for an ideal gas is 1 and from equation (10) and (12) density of the gas is:

$$\rho = \frac{n}{V_o} \tag{13}$$

Hence:

$$\rho = \frac{P}{ZRT} \tag{14}$$

R does not change when the composition of the gas is constant (Fox, 2004).

$$\frac{\partial \rho}{\partial \mathrm{t}} = \frac{1}{Z \cdot R} \frac{\partial}{\partial t}\left(\frac{P}{T}\right) \tag{15}$$

It should be noticed that the study fluid is real gases.

As it was explained before, the density rate must be defined in order to use the continuity equation. By using the relationship between density, temperature and pressure for real gases, if the variations of pressure and temperature over time are determined, the density rate will be estimated.

5.1.6 Newtonian Fluid

If relation between shear stress and strain rate curve is linear, this fluid will be classified as Newtonian fluid. For this type of fluid (Fox, 2004):

$$\tau_{ij} = \mu\left(\frac{\partial u_i}{\partial x_j} + \frac{\partial u_j}{\partial x_i}\right) \tag{16}$$

Where:

μ is dynamic viscosity of the fluid that is depends on pressure (temperature) of the fluid;

τ_{ij} is the shear stress created by the flow;

$\left(\frac{\partial u_i}{\partial x_j} + \frac{\partial u_j}{\partial x_i}\right)$ is velocity gradient perpendicular to the direction of the shear stress and it is equivalent to strain rate. Strain is a dimensionless quantity (m/m) therefore the unit of strain rate is sec^{-1}. The unit of velocity gradient is also sec^{-1}. Strain will be explained fortune.

Above equation, which defines the relation between fluid's velocity and shear force, is one of the main equations in order to develop the applied forces on a fluid particle.

It should be noted that above formula consists another term related to the velocity in the third direction. Since in this project the fluid is assumed to flow in one direction the third term is neglected.

This equation defines the relation between shear stress, velocity and viscosity of the fluid. It helps to find and develop a relation between fluid's pressure, applied body forces on the fluid, fluctuation of density and velocity over time. The mentioned relationship is represented further.

5.1.7 Applied Forces on a Fluid Particle

The Newton's second law is:

$$d\vec{F} = \frac{\partial}{\partial t}(mV) \tag{17}$$

Where $d\vec{F}$ is net force of the fluid. For an infinitesimal system with mass of *dm*:

$$d\vec{F} = dm\frac{d\vec{V}}{dt}\bigg|_{Sys} \Rightarrow d\vec{F} = dm\frac{D\vec{V}}{Dt} \tag{18}$$

$$dm = \iiint \rho\, dx\, dy\, dz \tag{19}$$

$$\frac{D\vec{V}}{Dt} = u\frac{\partial\vec{V}}{\partial x} + v\frac{\partial\vec{V}}{\partial y} + w\frac{\partial\vec{V}}{\partial z} + \frac{\partial\vec{V}}{\partial t} \tag{20}$$

Where $\vec{V}, V, u, v\ and\ w$ are filed velocity, total velocity, velocity in *X*, *Y* and *Z* direction, respectively. *Figure 5* shows a fluid particle in *X*-direction. If the stresses at the centre of the systems are σ_{xx}, τ_{yx}, τ_{zx}; the surface forces (dF_{Sx}) in *X*-axis can be developed as below.

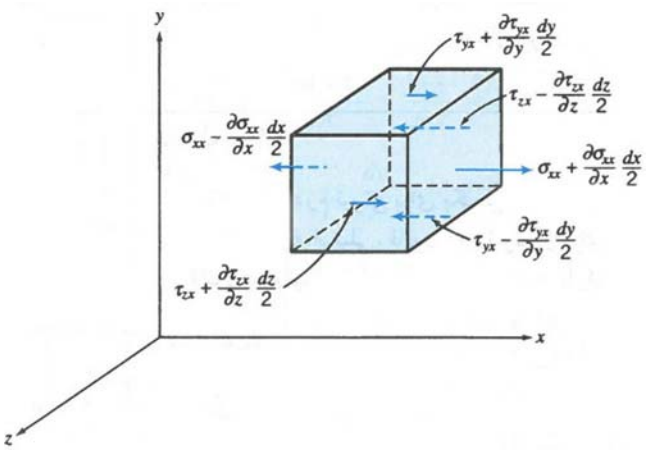

Figure 5. Stresses no a Fluid Particle in X-Axis Moody Diagram (Fox, 2004)

$$\begin{aligned} dF_{Sx} &= \left(\sigma_{xx} + \frac{\partial \sigma_{xx}}{\partial x}\frac{dx}{2}\right)dy\,dz - \left(\sigma_{xx} - \frac{\partial \sigma_{xx}}{\partial x}\frac{dx}{2}\right)dy\,dz \\ &+ \left(\tau_{yx} + \frac{\partial \tau_{yx}}{\partial y}\frac{dy}{2}\right)dx\,dz - \left(\tau_{yx} - \frac{\partial \tau_{yx}}{\partial y}\frac{dy}{2}\right)dx\,dz \\ &+ \left(\tau_{zx} + \frac{\partial \tau_{zx}}{\partial z}\frac{dz}{2}\right)dx\,dy - \left(\tau_{zx} + \frac{\partial \tau_{zx}}{\partial z}\frac{dz}{2}\right)dx\,dy \\ \Rightarrow dF_{Sx} &= \left(\frac{\partial \sigma_{xx}}{\partial x} + \frac{\partial \tau_{yx}}{\partial y} + \frac{\partial \tau_{zx}}{\partial z}\right)dx\,dy\,dz \end{aligned} \tag{21}$$

And if the only body force (dF_{Bx}) in *X* direction is the weight force, the total applying force on the fluid particle will be:

$$dF_x = dF_{Bx} + dF_{Sx} = \left(\rho g_x + \frac{\partial \sigma_{xx}}{\partial x} + \frac{\partial \tau_{yx}}{\partial y} + \frac{\partial \tau_{zx}}{\partial z}\right) dx\, dy\, dz \quad (22)$$

It is the acting forces in X-axis. With the same concept it can be developed for other directions (Fox, 2004).

By using the continuity equation and having Newtonian fluid concept in mind, the above equation leads to find the Navier-Stokes equation for a compressible flow (Tritton, 1988).

$$\frac{D(\rho \vec{V})}{Dt} = -\nabla P + \mu \nabla^2 \vec{V} + F_B \quad (23)$$

At the right hand side of the above formula, the first term is the pressure force; the second term is the viscose force and the third term is the body force. This equation specifies the relations between density, velocity, pressure, viscosity and the body force.

The OLGA solves one dimensional version of the continuity equation, the energy equation and the Navier-Stokes equation.

5.1.8 Pressure Drop

As it was explained before, the pressure at rupture point must be defined for identifying the other unknown properties. Since the pressure at the beginning point of the pipeline is known, it is needed only to evaluate pressure drop. Pressure drop specifies the differences between pressure at start point and pressure at the end point.

$$\Delta P = P_{end\ point} - P_{start\ point} \quad (24)$$

OLGA software needs the pressure at the ruptured section before the rupturing moment to being able to solve the equations. Due to steady state flow inside the pipe before rupture, the pressure drop can be calculated by using the below formula (Karunakaran, 2011):

$$\Delta P = \frac{f \rho V^2 L}{2 D_i} + \rho g H \quad (25)$$

Where *f* is Darcy-Weisbach friction factor which can be found by using the Moody Diagram shown in *Figure 6*. *H*, *L* and D_i are height difference between the desired points for single phase fluids, length of the pipeline and inner diameter of the pipeline, respectively.

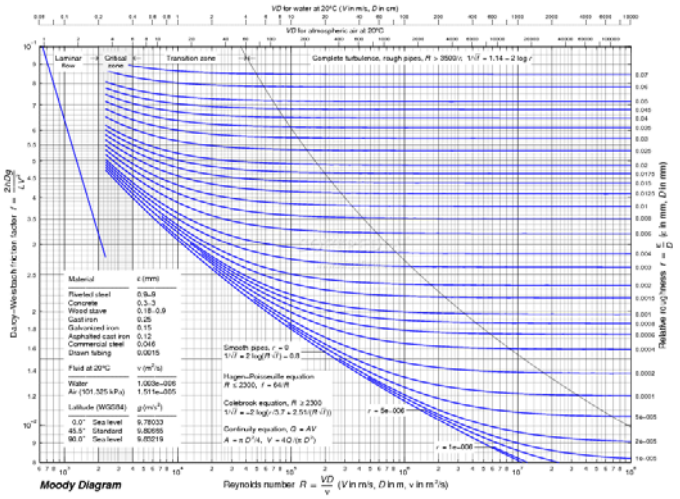

Figure 6. Moody Diagram (Fox, 2004)

To compute the velocity the mass flow rate must be known. According to the steady state flow and equation *(3)*, below formula is obtained to estimate the velocity (Fox, 2004).

$$V_o = \frac{\dot{m}}{\rho A} \tag{26}$$

Where A is the area of pipeline's cross-section.

5.1.9 Temperature at a specified point

Similar to the pressure, the temperature prior to the rupture must be evaluated in order to solve the other equations for the transient flow subsequent to the incident. One should define how the temperature changes along the pipe in the steady state flow. Temperature at a specified point inside the pipeline is computed with respect to concepts of heat transfer. This part is developed with respect to Hjertager (2011).

Each system exchanges work and heat with its surroundings. In this project the fluid inside the pipeline does not interact with the seawater by exchanging work and exchanging heat is the only mode of interaction. Thus, heat transfer and thermal properties are employed while the effect of ambient and pipeline has been taken into account.

Transferred thermal energy is heat transfer and it occurs due to temperature difference. The heat is always transferred from the higher temperature to lower temperature. In this project the temperature of fluid is higher than the temperature of surrounded seawater; therefore the heat transfer is from the fluid to the seawater. There are three modes of heat transferring and one must define which ones of them are occurred.

- Conduction heat transfer: If a temperature gradient exists through a solid or a stationary fluid, this mode of heat transfer must be considered. For a cylindrical tube as *Figure 7* shows, the value of conduction heat transfer flux $\left(\dot{Q}_{Cond,Cyl}\right)$ is expressed by below formula:

$$\dot{Q}_{Cond,Cyl} = -2\pi L \cdot K \cdot \frac{T_2 - T_1}{ln\left(\frac{r_2}{r_1}\right)} \quad (27)$$

Where:

L is the length of the pipe

K is the conductivity of the pipe

r_2 is the outer radius of the pipe

$r_1$is the inner radius of the pipe

T_2 is the temperature of the outer surface

$T_1$is the temperature of the inner surface

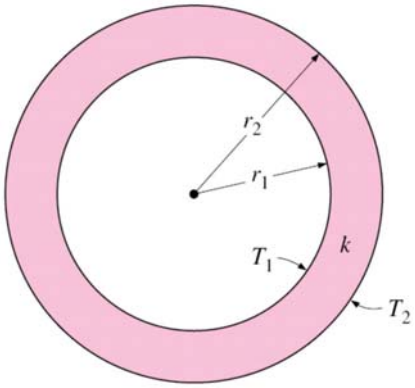

Figure 7. Configuration of Temperature Difference of the Pipe's Cross-Section (Hjertager, 2011)

The generated assumptions for this case are represented below:

There is no heat generation

The conductivity is constant

Heat conduction is one-dimensional

It should be mentioned that temperature of inner and outer surfaces are constant due to the steady state flow.

- Convection heat transfer: This mode occurs when a moving fluid is in touch with a solid surface or even between particles of a moving fluid. The convection heat transfer flux in the case of an interaction between a moving fluid and a solid surface is defined by:

$$\dot{Q}_{Conv} = h \cdot A_s \cdot \Delta T \quad (28)$$

Where A_s is the contact surface area, ΔT is temperature difference and h is the convection heat transfer coefficient of the fluid. It should be noticed that for steady state flow the h is constant and for a circular tube cross-section, it is estimated by:

$$h = \frac{K}{D} \cdot N_u \quad (29)$$

$$\dot{Q}_{Cond} = h \cdot A_s \cdot \Delta T \quad (30)$$

where D is the inside diameter for the fluid inside the pipe and outer diameter for the seawater. In addition, the N_u is the Nusselt number. If it is assumed that Reynolds number (R_e) is higher than 10,000 and Prandtl number (P_r) is between $0{,}7$ and 160, then the evaluation of the N_u is expressed by:

$$N_u = 0{,}0023 \cdot {R_e}^{0{,}8} \cdot {P_r}^{n} \begin{vmatrix} n = 0{,}4\ heating \\ n = 0{,}3\ cooling \end{vmatrix} \quad (31)$$

The R_e for a circular cross-section is evaluated by:

$$R_e = \frac{\rho \cdot V \cdot D}{\mu} \quad (32)$$

And P_r is evaluated by the below equation:

$$P_r = \frac{\mu C_P}{k} \quad (33)$$

Where the C_P is specific heat capacity of the fluid. The typical range of the P_r for gases is between $0{,}19$ & $1{,}0$ while for the water it is between $1{,}19$ & $13{,}7$.

- Thermal radiation: This case happens when there is no contact between surfaces. For this mode to be significant compared to convection and conduction modes the temperature must be high. In this study case the temperature is low; therefore, its details will not be covered by this project. For more info see Hjertager (2011).

According to explained modes as well as the conditions of this project only the conduction and convection are considered. As it is displaced by *Figure 8*, the study case is a multi-layered cylinder where gas flows inside the pipe while the seawater current interacts with the outer surface of the pipeline.

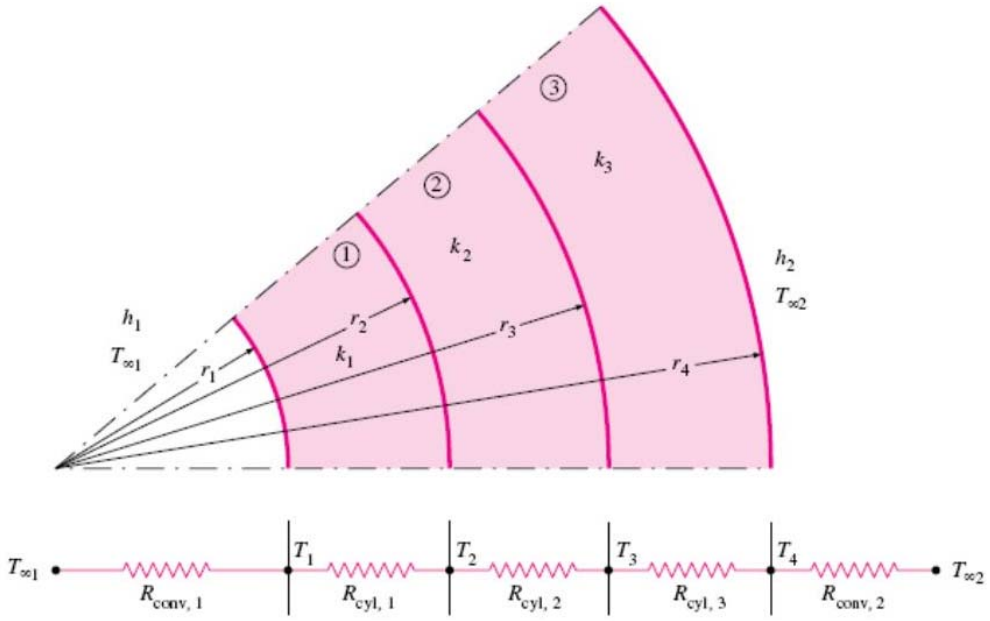

Figure 8. Heart Transfer Model of a Multilayered Cylinder (Hjertager, 2011)

With respect to the above figure and the study case, the first layer is made by steel, the second layer is made by anti-corrosion and the last layer is the concrete layer. The h_1 & $T_{\infty 1}$are the heat transfer coefficient and the temperature of the fluid, respectively. The h_2 is the heat transfer coefficient of the seawater and $T_{\infty 2}$ is the ambient temperature. One should notice that the temperature is altered along the pipe but it is constant over time. It is common to use resistance for modeling the total heat transfer flux $(\dot{Q}_{tot})$; hence:

$$\dot{Q}_{tot} = \frac{T_{\infty 1} - T_{\infty 2}}{R_{tot}} \tag{34}$$

Where R_{tot} is the total modelled heat resistance and in this case it is expressed as:

$$R_{tot} = \frac{1}{(2\pi r_1 l)\cdot h_1} + \frac{ln\left(\frac{r_2}{r_1}\right)}{2\pi l \cdot k_1} + \frac{ln\left(\frac{r_3}{r_2}\right)}{2\pi l \cdot k_2} + \frac{ln\left(\frac{r_4}{r_3}\right)}{2\pi l \cdot k_3} + \frac{1}{(2\pi r_2 l)\cdot h_2} \tag{35}$$

Based on the above equations the $\dot{Q}_{tot}$ along the pipe can be computed. Since the aim is to define the temperature at an interested point (rupture point); another equation that relates the temperature at the beginning section of the route and the rupture point is needed. This equation which determines the temperature difference between two interested points is presented below:

$$T_e - T_i = \frac{\dot{Q}_{tot}}{\dot{m}\cdot C_P} \tag{36}$$

As the *Figure 9* shows the T_e is the temperature at the end cross-section (required cross-section) and the T_i is the inner temperature at the beginning pipe's cross-section. In this case the T_i is known and the aim is to estimate the T_e.

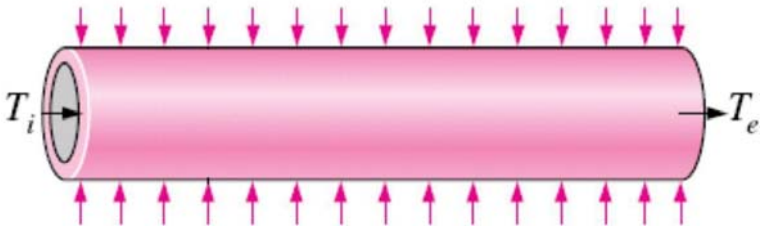

Figure 9. Heat Transfer Flux along a Pipe (Hjertager, 2011)

5.2 Mechanics of materials

When a dragging anchor hits a submarine pipeline and pulls it, it applies a load to the pipe. There are two scenarios that can rupture the pipeline. First one occurs due to absorbing a large impact load by the pipe and second one happens due to pull-over/hooking load. This project studies the second case. After the impact, the pipeline is pulled by the anchor and exceeding longitudinal strain above a specified limit causing the rupture.

In this case, although resisting forces due to the seabed friction try to prevent pipeline to moved, the anchor load is strong enough to bend and rupture the pipeline. In order to predict maximum pipeline's deflection it is necessary to estimate longitudinal strain of the pipeline just before rupturing. To achieve this purpose a solution is to examine the response of the pipeline's cross-section to the hooking load from the impact to the rupturing moment. In this project investigation of the pipeline's cross-section is mainly based on DNV's standards (2010a; 210b), and the Strain-Stress curve developed by Boresi A.P. and Schmidt (2003).

5.2.1 Strain-Stress Engineering Diagram

The diagram that is shown in *Figure 10* must be completely understood in order to solve the problem and define the response of the pipeline's cross-section to the external loads.

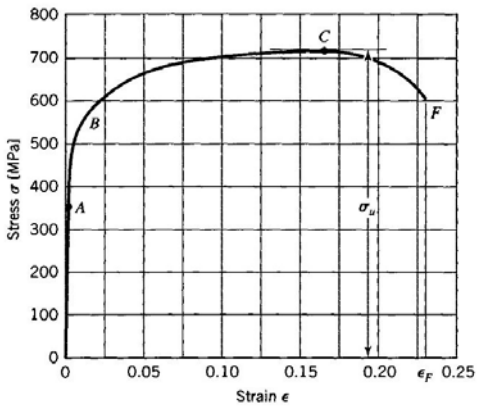

Figure 10. Engineering Strain-Stress Diagram for Tension Specimen of Alloy Steel (Boresi, 2003)

The length of a pipe section will increase if the pipe section is subjected to a tensile load (P_T). The increased length depends on the material as well as the magnitude of the load. The difference between the new length and the initial length is called elongation.

$$e = L_{new} - L_{initial} \tag{37}$$

Another important term is strain that is the ratio of elongation to the initial length of the member.

$$\varepsilon = \frac{e}{L_{initial}} \tag{38}$$

Elastic limit is maximum strain at which after unloading the bar, the final strain goes back to zero and the linear elasticity area is the region that a linear relationship between stress (σ) and strain exists (this region is illustrated in *Figure 10* from O to A).

$$\sigma = E \cdot \varepsilon \tag{39}$$

Where the constant in the above equation is known as modules of elasticity (E). If the strain exceeds the elastic limit, there will be a permanent strain (ε_p) in the bar even after unloading. In this case the bar experiences two different strains; True strain (ε_T) that occurs at loading moment and the permanent strain that occurs after removing the load. For example, point J in *Figure 11* is an arbitrary point for this case.

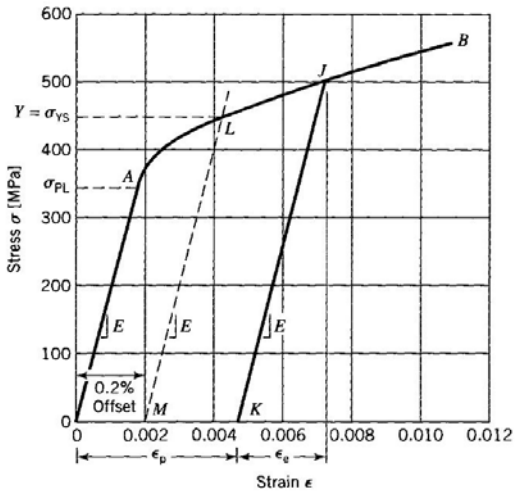

Figure 11. Engineering Strain-Stress Diagram for Tension Bar of Steel- expanded Strain Scale (Boresi, 2003)

The difference between ε_T and ε_p is known as elastic strain (ε_e).

$$\varepsilon_e = \varepsilon_T - \varepsilon_p \tag{40}$$

The agreed value for elastic strain is also called the offset value, or $0.002\ (0.2\%)$ of ε_p.

Yield stress (σ_Y) is defined by the interaction point between the strain-stress curve and the drawn line with the slope equalling *E* from the offset strain value point in strain axis. The stress at point *L* in *Figure 11* is the yield stress in this case.

Ultimate stress (σ_U) is the maximum stress in the stress-strain engineering diagram and in *Figure 10* it is shown by point *C*. The ability of materials that allows them to tolerate more stress beyond yield

stress with resisting of increasing strain is known as strain hardening effect. Additionally, it dominates beyond point C in *Figure 10*. The cross-section area decreases while the elongation is increased by the load. Area reduction decreases the ability of the material to withstand more than the ultimate tensile stress. This effect is known as softening effect and it dominates after point *C*.

At point *F* in *Figure 10* the bar will not be lengthened anymore and it will break. This point is known as rupture point and percentage elongation is the strain value at this point (Boresi, 2003). Thus, in order to define when rupture occurs one must identify the percentage elongation for the used material to fabricate the pipeline. As it was assumed, the pipeline was built by steel *X650*. Form *Figure 12* it can be construed that the percentage elongation of steel *X650* is around 24%.

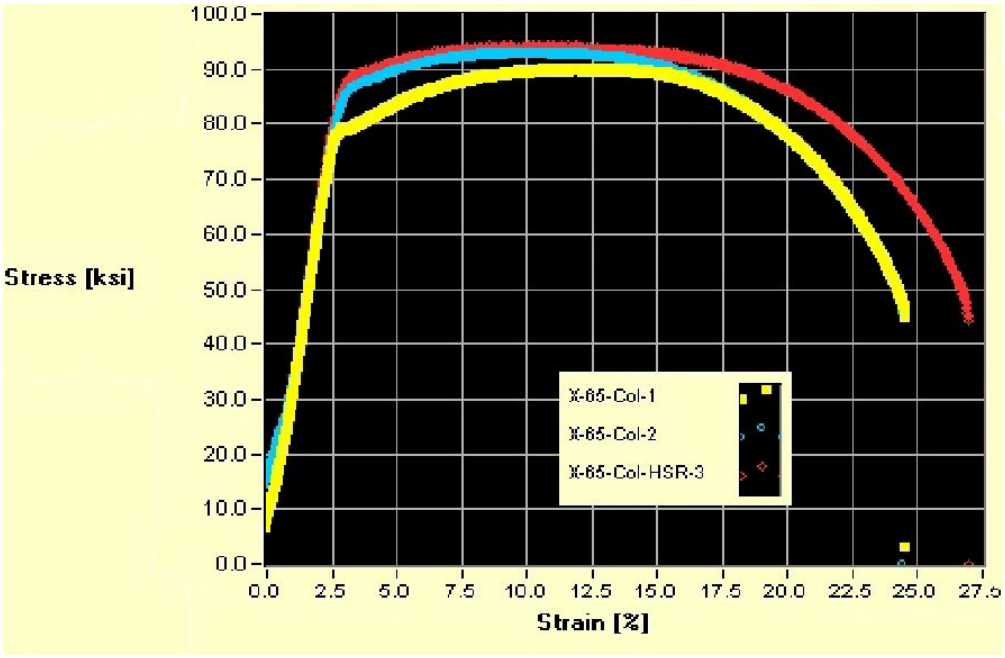

Figure 12. Engineering Strain-Stress Diagram of Steel X65 (Haggag, 1999)

Since the relation between stress and strain in the interested region is nonlinear and the percentage elongation is more than strain in the case of fully plastic region (area that all the cross-section area is in plastic region and there is no area that still is in elastic area) this value is found empirically. Therefore, in this project the calculation of the strain as well as the deflection of the pipe are carried out with ANSYS.

5.2.2 Pull-Over/Hooking Criteria

Although the needed strain for rupture of a tensile bar is around 24%, for a pipeline with respect to DNV (2010a) it can be less than 24%. The main damage due to pull-over/hooking loads is buckling and if it is developed it can rupture the pipeline (DNV, 2010b); thus the criteria of pull-over/hooking loads must be considered to define the value of strain that leads to tearing the pipe.

There are two criteria for surveying the case:

- Load Controlled condition (LC condition)

- Displacement Controlled condition (DC condition)

In this project the DC condition is used. In this method the design compressive strain for pipe sections subjected to bending moment, axial force and over pressure is defined by below equation:

$$\varepsilon_{Sd} \leq \varepsilon_{Rd} = \frac{\varepsilon_c(t_2, P_{min} - P_e)}{\gamma_\varepsilon} \, , {}^{D_{out}}/_{t_2} \leq 45, P_i \geq P_e \quad (41)$$

Where:

ε_{Sd} is design compressive strain and it is calculated by:

$$\varepsilon_c(t_2, P_{min} - P_e) = 0.78 \cdot \left(\frac{t}{D_{out}} - 0.01\right) \cdot \left(1 + 5.75 \cdot \frac{P_{min} - P_e}{P_b(t)}\right) \cdot {\alpha_h}^{-1.5} \cdot \alpha_{gw} \quad (42)$$

ε_{Rd} is design resistance strain;

P_{min} is the minimum internal pressure;

γ_ε is the strain resistance factor and *Table 5* is used to define its value.

Table 5. Resistance Strain Factor (DNV, 2010a)

Safety Class		
Low	Medium	High
2.0	2.5	3.3

α_h is minimum strain hardening and for steel *X65* is $0{,}93$ (DNV, 2010a)

α_{gw} is Girth weld factor and will be specified by using *Figure 13*.

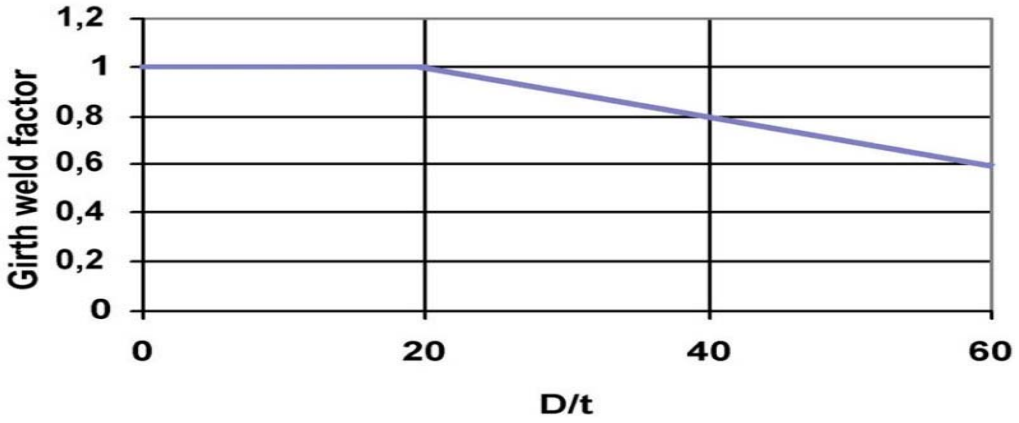

Figure 13. Proposed Girth Weld Factor (DNV, 2010a)

t is the steel wall thickness;

D_{out} is the outer diameter;

$P_b(t)$ is the pressure containment resistance which estimated by using below equations:

$$P_b(t) = \frac{2t}{D_{out} - t} \cdot f_{cb} \cdot \frac{2}{\sqrt{3}} \quad (43)$$

and f_{cb} is determined by:

$$f_{cb} = Min\left[f_y; \frac{f_u}{1.15}\right] \quad (44)$$

In addition, f_y and f_u are yield and tensile stress to be used in design, respectively. They are evaluated by below equations:

$$f_y = \left(\sigma_Y - f_{y.temp}\right) \cdot \alpha_u \quad (45)$$

$$f_u = \left(\sigma_U - f_{u.temp}\right) \cdot \alpha_u \quad (46)$$

Where:

$f_{y.temp}$ is de-rating on yield stress to be used in design;

$f_{u.temp}$ is de-rating on tensile strength to be used in design;

α_u is material strength factor and *Table 6* is used in order to define its value.

Table 6. Material Strength Factor (DNV, 2010a)

Factor	Normally	Supplementary requirement U
α_u	0,96	1,00

By using the mentioned equations and relations the ε_{Rd} will be estimated. The ε_{Rd} determines the limit of the strain that allows to occur. If the strain exceeds the ε_{Rd}, the pipeline will fail or rupture. In other words by estimating the ε_{Rd}, the minimum required strain causing rupture is specified. The relevant computations are presented in appendix C.

5.2.3 Local Buckling/Collapse Criteria

The boundary conditions of the pipeline before rupture are different from the pipe's shape post rupture. Due to the differences the used theory must be changed. In order to determine the destroyed length of the pipeline due to the pushing force applied by the escaped fluid, one must examine the pipe's condition with validated criteria.

Since the pipeline was already bent, the axial and compressive force applied at ruptured cross-section will create a bending moment. This bending moment bends the pipeline and the pipe will collapse due to buckling. Thus, in this study the local buckling/collapse criteria are used to identify the damaged length. Local buckling refers to gross deformation of pipe's cross-section which could

be due to external pressure, bending moment or combined loading (DNV, 2010a). The used method in this section is mostly based on Hauch and Bai (2000).

Latest research results show that nonlinear finite element method is accurate enough to predict the strength capacity of pipes (Hauch, 1998). One of the useful characteristics for analysing the local buckling/collapse phenomena is moment-curvature relationship. The challenge in this case is the curvature illustrated by *Figure 14* which can only be obtained by doing laboratory tests or using the finite element method (Hauch, 1998).

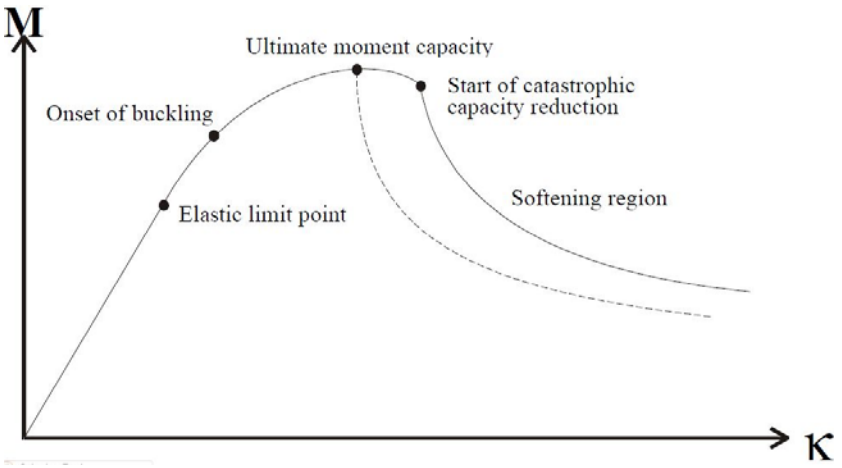

Figure 14. Typical Moment Curvature Relationship for Pipe under Constant Pressure and Axial Force (Hauch, 2000)

Consider a straight pipe which is loaded by internal pressure and longitudinal force as well as subjected to bending; thus its curvature increases. At first the pipe's cross-section will be in the linear limit region where the shape of the cross-section does not permanently change. After exceeding the linear limit area there will be a permanent change in the shape of the cross-section.

By increasing curvature more the cross-section will reach the point at the onset of buckling. Imperfect geometry and/or imperfect material influence the buckling point location on the diagram. One should notice that at small curvature levels the ultimate moment capacity is not highly affected.

As the cross-section continues to change after the onset of buckling point, bending energy is increasingly accumulated. This accumulation continues until ultimate moment capacity is reached and where the geometrical collapse occurs.

From the ultimate moment capacity to the start of catastrophic capacity reduction point the geometric collapse occurs slowly and the changes of the pipe's cross-section area could be neglected.

Softening region begins after the start of catastrophic capacity point and the pipe's cross-section collapses.

It must be mentioned that if a bending moment is applied to the pipe, the start of catastrophic capacity reduction will happen exactly after the ultimate moment capacity. This condition is shown by dashed line in the *Figure 14* (Hauch, 2000).

The moment checking criterion is the yielding criterion in case of combined loading (internal pressure with bending moment). The maximum moment capacity of the pipe is measured to define whether it is in the safe region or not. The pipe's cross-section reaches to its maximum moment capacity if the entire cross-section yields. It should be noticed that in this situation the strain will be $0{,}5\%$ (Hauch, 1998).

Due to the complexity of the analytical method developed by Hauch (2000) the finite element method which has the potential to give a proper answer is used in this project. The finite element method subdivides the created model into specified mesh elements and nodes. After that the behaviours of the mesh elements are estimated and then obtained results are used for further analysis.

To utilize the finite element method two main assumptions are required:

- residual stresses are negligible
- the effects of the welding cross-sections between two pipe sections are not considered

The reason for emphasising assumptions is that the residual stresses and welded cross-sections may cause that buckling occurs earlier.

Beside the assumptions it is necessary to take care of:

- define the boundary conditions
- a proper expression of the conservative law of the pipe material
- a suitable load sequence
- ability of considering large deflection, large rotation and finite strain
- ability of computing all relevant failure modes (Hauch, 2000)

With respect to the used theories as well as mentioned assumptions, the software, OLGA and ANSYS, are used to model the case and analysis will be carried out.

6 Analyses and Results

Based on the explained used theory, the analysis is divided into five steps. These five steps are summarized and represented as below:

- Analysis of steady state flow before rupture to define the interaction between fluid and the pipeline before rupture and also its effect on the fluid condition after rupture. This step is analysed by using OLGA.
- Analysis of transient flow after rupture in order to identify the thrust force due to escaping gas jet. This step is analysed by using OLGA.
- 3-D finite element analysis of pipeline under anchor load in order to determine the initial deformed shape at rupture moment. The analysis of this step is carried out by using ANSYS.
- 3-D finite element analysis of pipeline after rupture. Result of this step determines the final deformed shape of the pipeline. ANSYS is used in this step.
- Evaluation of the final deformed shape of the pipeline in order to identify the damaged length of the pipeline.

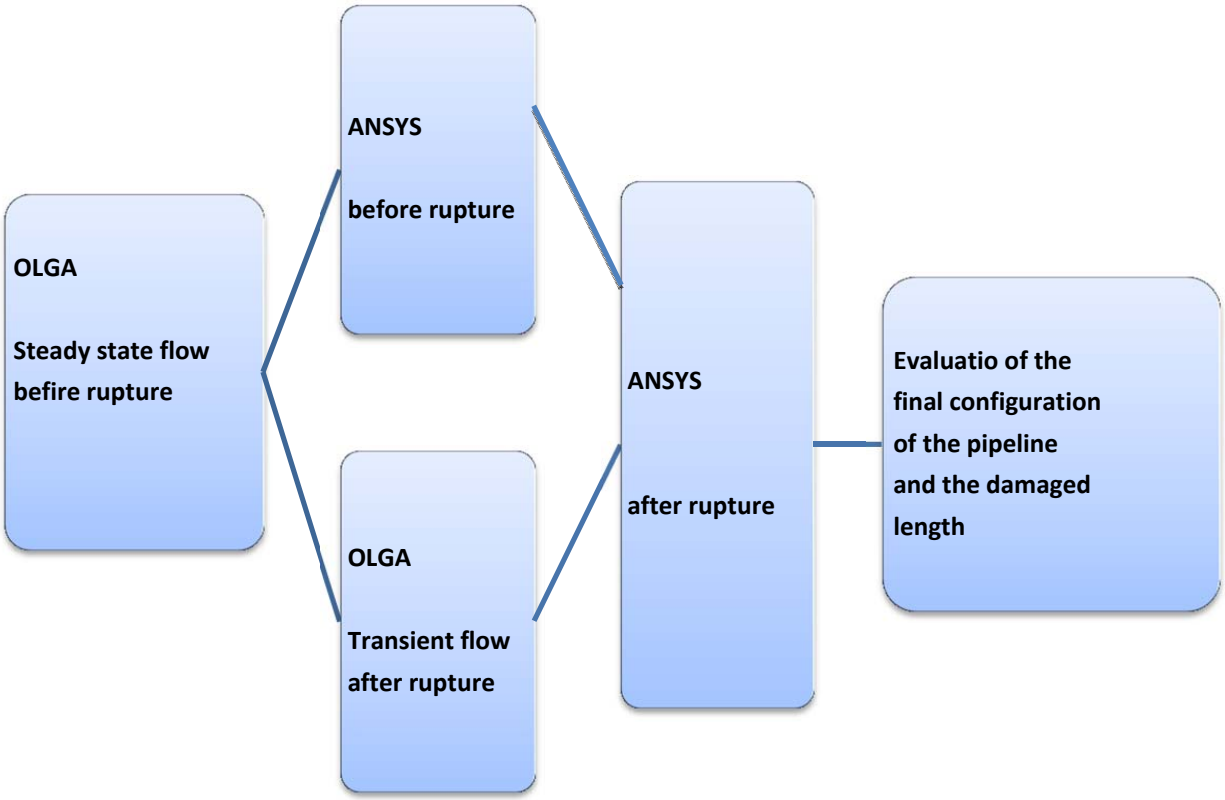

6.1 OLGA

OLGA software is used to define which pipeline section will encounter the maximum fluid jet induced thrust force if a full bore rupture occurs. Not only will it help to compute maximum mass flux, but it also identifies variations of density, temperature and pressure of the fluid over time pre and post rupture.

Due to long length of the subsea pipeline, it was suggested to focus only on one section of the pipeline. It should be reminded that the aim of this project is to study the worst case scenario. Thus the proper section to study is the section which is encounters the maximum thrust force due to released fluid. Since the applied force from the leak is proportional to the mass flux out of it, the pipe section with maximum flow rate will lead to the maximum force. Therefore, OLGA was used to calculate the mass flow rate of a full bore leak from each pipe section separately to identify interested pipe section. Therefore, OLGA was run 24 times and in each step, rupture occurs in only in one pipe section.

6.2 Input Data

OLGA demands various information related to the environmental conditions and the pipeline route in order to be run. The necessary information is listed below.

Local current velocity (Seawater)	: 0,1 $^{m}/_{s}$
Initial internal pressure	: 220 $barg$
Initial internal temperature	: 20 ℃
Outside temperature	: 7 ℃
Standard steady state flow rate	: 84 $Mill\ ^{sm^3}/_{d}$

It should be mentioned that for each part of the pipeline, the outside pressure is unique due to different elevation of each section. Thus in this project the average of outside pressure is used and the average pressure is calculated by estimation of average height of each section and multiplying it by the water density and earth's gravity. In addition, the used material and their wall thickness are according to *Table 4* and internal and external coating (see chapter *3*- section *8*).

6.3 Results of OLGA

With respect to all the noted conditions and assumptions, OLGA was run for each case of rupture.

In this project it is assumed the incident occurs after 24 hours of steady state and with the leak openly in one second.

As it shown by *Table 7* and *Figure 15*, the peak leak flow rate is $35895.11\ kg/s$ and occurs at *KP090*. Therefore, the further investigation will be done only for pipe section *KP090*. *Figure 16* shows the mass flow rate over time. The other analysis in order to estimate the created force due to the leakage of the gas is presented in *Appendix B*.

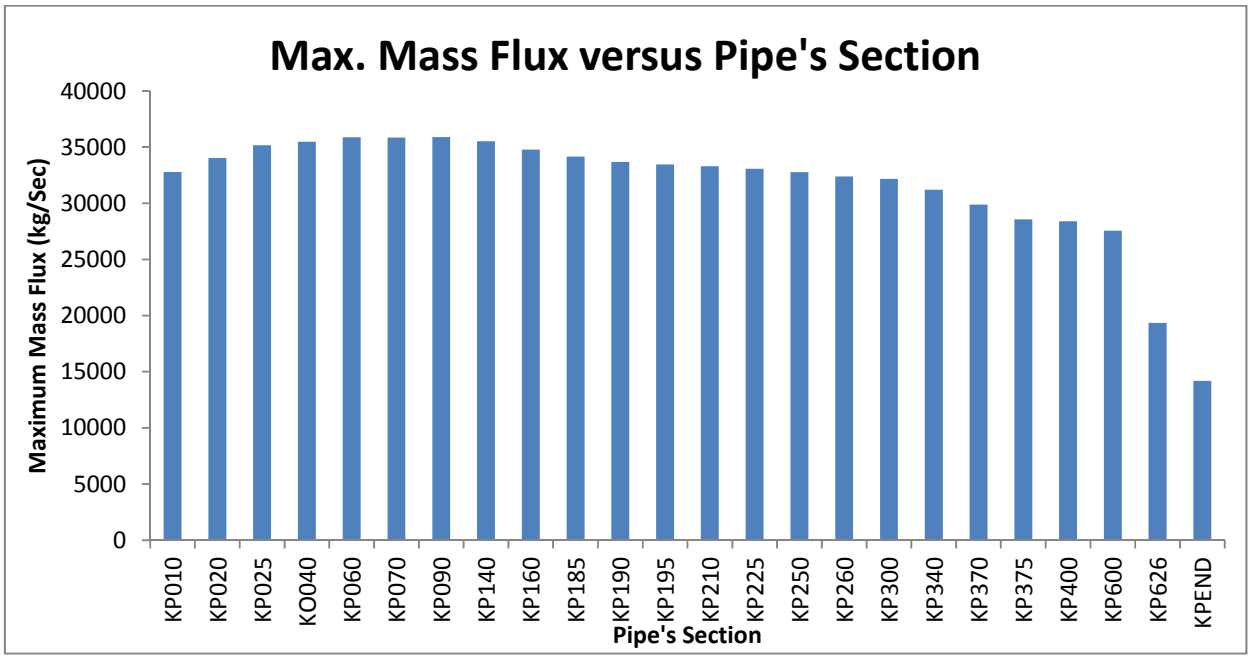

Figure 15. Maximum Mass Flux versus Pipe's Section

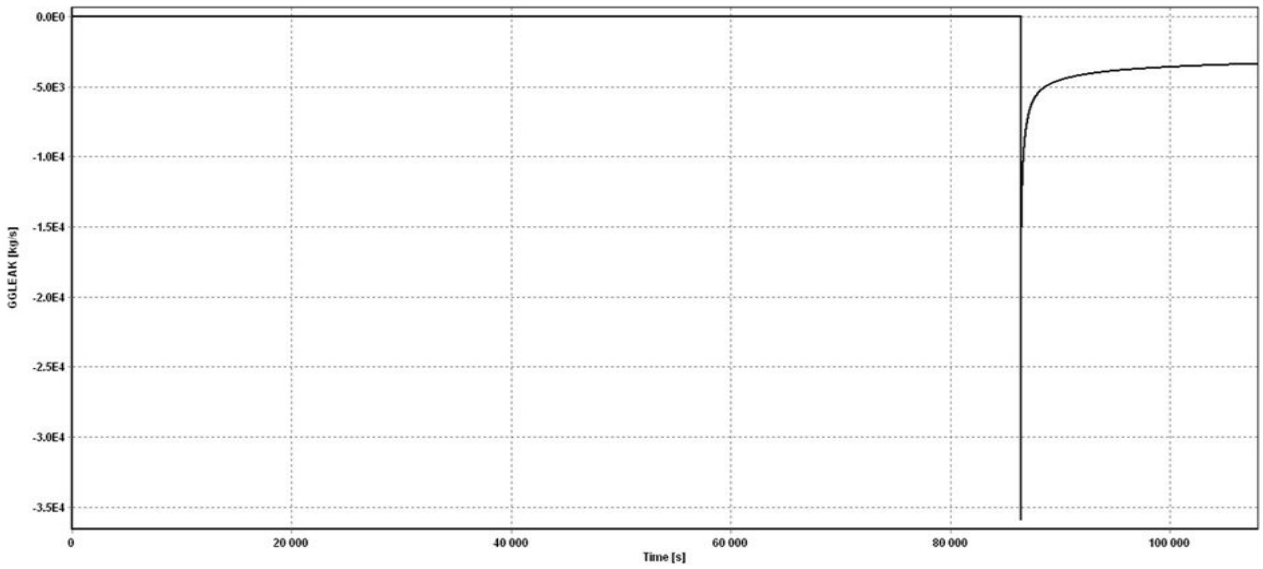

Figure 16. Mass Flow Rate of KP090 over Time

Table 7. Peak Leak Mass Flow Rates of Pipe Sections

Section of the Pipeline	Peak Leak Mass Flow Rate (Kg/s)
KP010	32789.44922
KP020	34016.14844
KP025	35177.23828
KP040	35482.94141
KP060	35871.71094
KP070	35850.62891
KP090	35895.10938
KP140	35513.55859
KP160	34780.94141
KP185	34157.69141
KP190	33690.01172
KP195	33454.67188
KP210	33299.35156
KP225	33063.69922
KP250	32771.10938
KP260	32386.14063
KP300	32176.71094
KP340	31204.58008
KP370	29874.4707
KP375	28564.84961
KP400	28391.74023
KP600	27565.18945
KP626	19346.68945
KPEND	14192.01953

6.4 Finite Element model and results – before Rupture

In order to achieve the main goal which is defining the response of the pipeline to the rupture leak to predict damaged length; it is necessary to know the pipeline's configuration just before the rupture. To specify the deformation of the pipe due to the applied load by the anchor in this project, finite element method is used. A pipe with length of $3000\ m$ is modelled and analysed with ANSYS 14.

After creating the pipeline's model and applying the boundary conditions, the anchor forces were imposed at the middle of the pipeline. According to the result computed in *Appendix C* the minimum strain to get a rupture was $5{,}25\%$; therefore, the aim was to find the deformation of the pipeline where strain of the pipe's cross-section at the middle of the pipe is just exceeding $5{,}25\%$. This project

studied a case where the strain in the middle of the pipe reaches $7{,}18\%$, a strain well above the desired limit given above.

Due to the long length of the model $(3000\ m)$ the initial number of mesh elements was many; thus, it was decided to reduce the number either by reducing the length of the pipe section, creating coarse mesh, or by eliminating the concrete and anti-corrosion layers. The model must contain a long enough pipeline to give a reliable result; therefore, reducing the length of pipe was not chosen. Another alternative solution was creating coarse mesh elements. This solution showed to an undesirable reduction in the accuracy of the result. Since differences between the strength of the steel and concrete and anti-corrosion are large enough that the removing layers will not significant affect the results; it was decided to remove the concrete and anti-corrosion layers.

The effects of temperature differences are neglected due to the low temperate differences between fluid inside the pipe and the seawater surrounded the pipeline.

Inside and outside pressures as calculated the OLGA were applied to the model (see *Appendix B*). According to the assumption that the extremities of the pipe will not move, fixed supports were used in order to prevent the ends of the model to move.

Twenty nine similar springs (Body to Ground) were used to model the force of the friction between soil and pipe. It should be mentioned that the force due to springs are not constant. The applied force due to a linear spring is proportional to the elongation of the spring.

$$F_s = K_{sp} \cdot X_s \tag{47}$$

Where F_s is the resisting force of the spring, K_{sp} is the stiffness of the spring and X_s is the elongation of the spring. As it is seen, if the stiffness is constant, the F_s increases while the spring is elongated. One must notice that the resisting forces due to the interaction of soil and the pipeline are almost constant for large deflection. Thus, in order to apply constant resisting forces to the pipeline it was necessary to reduce the stiffness while X_s is increasing. However the default setting of spring in ANSYS Workbench 14 is linear spring (constant stiffness). Therefore, ANSYS Parameter Design Language (APDL) commands were used to change the stiffness according to elongation for applying constant resisting forces; or in other words by using the APDL commands the linear springs became non-linear springs. Summary of written APDL commands is presented in *Appendix D*.

To define the stiffness of the springs, the model was split into thirty even sections with $100\ m$ length. Then it was assumed that the average of the deformation of each point along each section is same as the deformation of the middle point of that pipe's section. Thus the springs were applied at the middle of the pipe's sections where each spring covered $100\ m$ of the pipe. Based on the explanation and the resisting forces on the pipeline, $207900\ {}^{kN}/_{m}$ was chosen for the initial stiffness of each spring. After that the related APDL commands were written that reduced the stiffness for each $10\ m$ elongation. The concepts, used formulas, hand calculations and related stiffness for each elongating of the springs are represented in *Appendix D*.

Table 8 presents the location and the covered area of the used springs.

Table 8. Location and Covered Area of the Used Springs in the Prior to Rupture Model

Number of Spring	Location of Spring (m)	Covered Area (m)	Number of Spring (m)	Location of Spring (m)	Covered Area (m)
1	50	100	16	1550	100
2	150	100	17	1650	100
3	250	100	18	1750	100
4	350	100	19	1850	100
5	450	100	20	1950	100
6	550	100	21	2050	100
7	650	100	22	2150	100
8	750	100	23	2250	100
9	850	100	24	2350	100
10	950	100	25	2450	100
11	1050	100	26	2650	100
12	1150	100	27	2750	100
13	1250	100	28	2850	100
14	1350	100	29	2950	100
15	1450	100			

In order to mesh the model one *Mapped Face Meshing* and one *Edge Sizing* were used for the pipe's cross-section; the details are shown in *Table 9* and *Table 10* , respectively.

Table 9. Details of "Mapped Face Meshing" - Mapped Face Meshing

Scope	
Scoping Method	Geometry Selection
Geometry	1 face
Definition	
Suppressed	No
Radial Number of Divisions	2
Constrain Boundary	No

Table 10. Details of ''Edge Sizing'' - Sizing

Scope	
Scoping Method	Geometry Selection
Geometry	2 Edges
Definition	
Suppressed	No
Type	Number of Divisions
Number of Divisions	20
Behaviour	Hard
Bias Type	No Bias

The whole body was meshed by utilizing the *Sweep Method* and *Table 11* shows the related details.

Table 11. Details of ''Sweep Method'' - Method

Scope	
Scoping Method	Geometry Selection
Geometry	1 Body
Definition	
Suppressed	No
Method	Sweep
Element Midside Nodes	Use Global Setting
Src/Trg Selection	Automatic
Source	Program Controlled
Target	Program Controlled
Free Face Mesh Type	All Quad
Type	Element Size
Sweep Element Size	5, m
Sweep Bias Type	No Bias
Element Option	Solid

With respect to the used mesh methods the elements and nodes are 24000 and 132160, respectively. More details are represented by *Table 12*.

Table 12. Details of ''Mesh''

Defaults		**Sizing**		**Inflation**		**Advanced**		**Defeaturing**	
Physics Preference	Mechanical	Use Advanced Size Function	Off	Use Automatic Inflation	None	Shape Checking	Standard Mechanical	Pinch Tolerance	Please Define
Relevance	0	Relevance Centre	Coarse	Inflation Option	Smooth Transition	Element Midside Nodes	Program Controlled	Generate Pinch On Refresh	No
Statistics		Element	Default	Transition Ratio	0,272	Straight Slide Elements	No	Automatic Mesh Based Defeaturing	On
Nodes	132160	Initial Size Seed	Active Assembly	Maximum Layers	5	Number Of Retries	Default (4)	Defeaturing Tolerance	Default
Elements	24000	Smoothing	Medium	Growth Rate	1,2	Extra Retries For Assembly	Yes	**Patch Conforming Option**	
Mesh Metric	None	Transition	Fast	Inflation Algorithm	Pre	Rigid Body Behaviour	Dimensionally Reduced	Triangle Surface Mesher	Program Controlled
		Span Angle Centre	Coarse	View Advanced Option	No	Mesh Morphing	Disabled		
		Min. Edge Length	3,1919 m						

Figure 17 and *18* show the 3-D meshed model from different views.

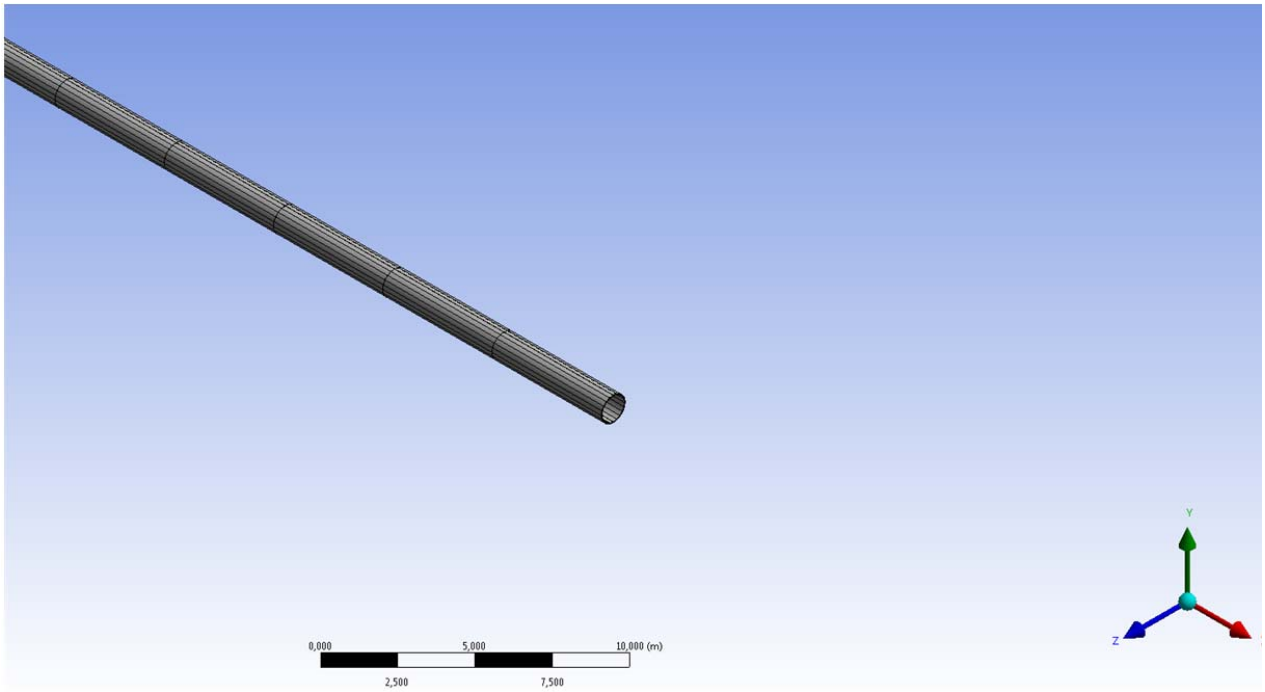

Figure 17. 3-D meshed model

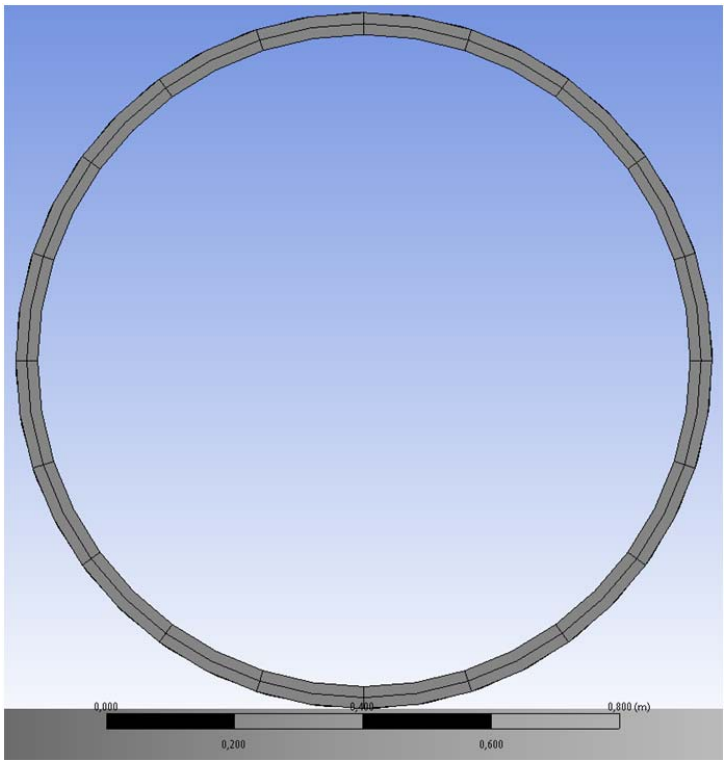

Figure 18. 3-D meshed model of Pipe's Cross-Section

To compute the total deformation and equivalent elastic strain of the model for desired points, a path was identified. The path was created from the beginning point of the mode due to the symmetry of the model.

The large deflection was considered in the analysing setting and other details of the analysing setting are shown by *Table 13*.

Table 13. Details of ''Analysis Setting''

Step Controls		**Solver Controls**		**Nonlinear Controls**	
Number Of Steps	1,	Solver Type	Program Controlled	Force Convergence	Program Controlled
Current Step Number	1,	Weak Springs	Off	Moment Convergence	Program Controlled
Step End Time	1, s	Large Deflection	On	Displacement Convergence	Program Controlled
Auto Time Stepping	On	Inertia Relief	Off	Rotation Convergence	Program Controlled
Define By	Sub Steps	**Restart Controls**		Line Search	Program Controlled
Initial Sub Steps	1000,	Generate Restart Points	Program Controlled	Stabilization	Off
Min. Sub Steps	1,	Retain Files After Full Solve	No		
Max. Sub Steps	30000				

SOLID185 that is utilized for *3-D* modelling of solid structure was chosen as required element type. It is described by 8 nodes and each node has three degrees of freedom. *Figure 19* displays the homogeneous structural solid geometry of *SOLID185*.

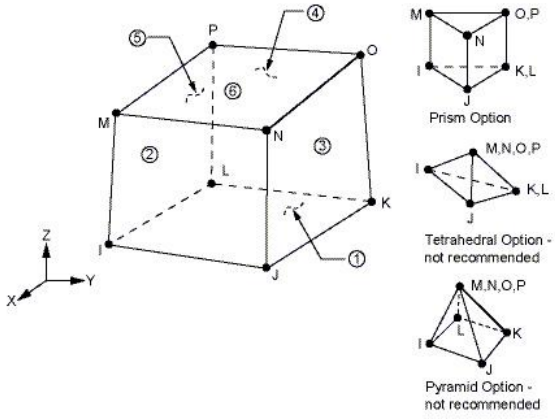

Figure 19. SOLID185 Homogeneous Structural Solid Geometry (ANSYS Workbench 14)

Figure 20 shows the 3-D finite element model juts before running the ANSYS.

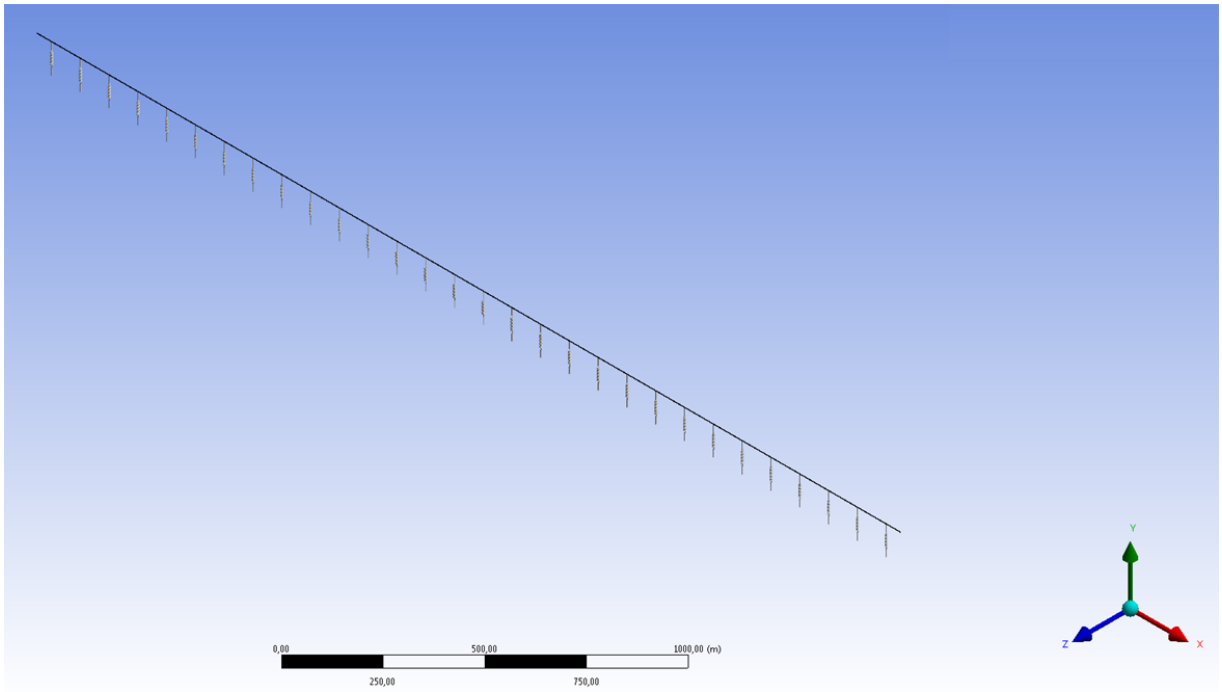

Figure 20. Pipe's model before running the ANSYS

Based on the mentioned settings the ANSYS was run to define the total deformation of the pipeline where the strain of the pipe's cross-section at the middle point reached to $7{,}18\%$. *Figure 21*, *Figure 22* and *Figure 23* show the strain, the total deformation along the pipe and the 3-D total deformation of the pipeline, respectively. It should be mentioned that due to the symmetry condition only information of one half of the pipe was gathered for the strain.

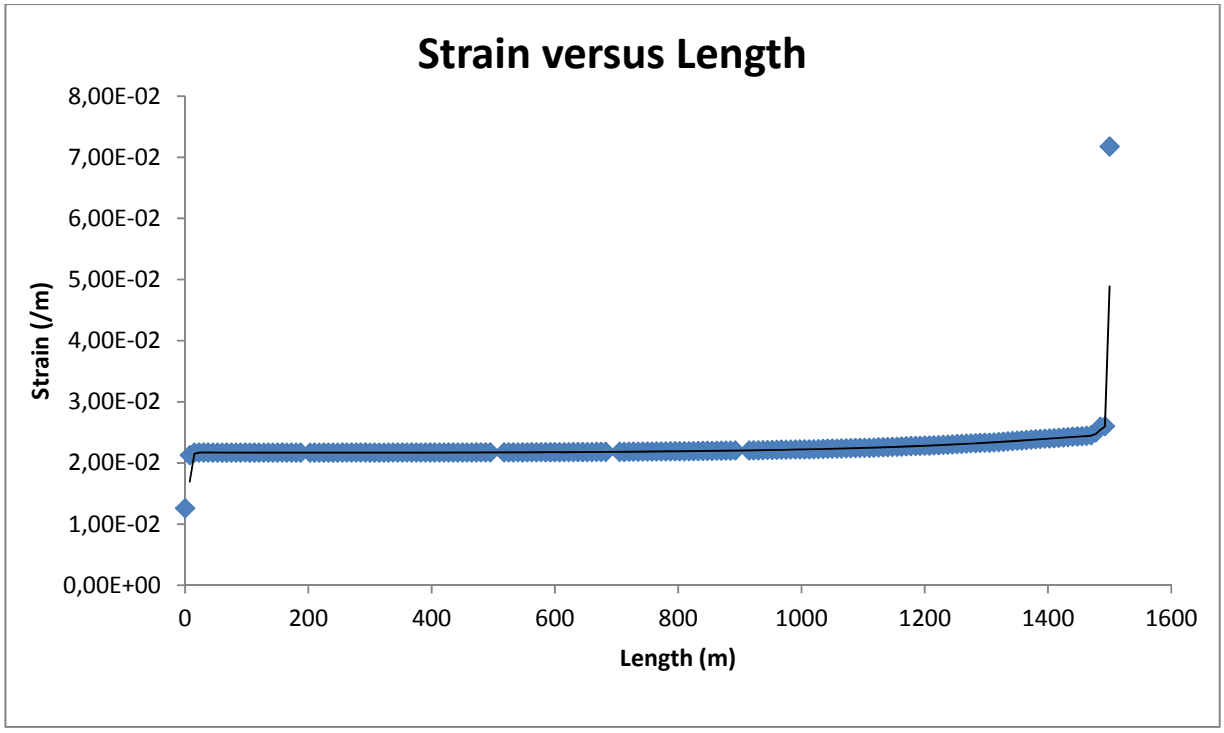

Figure 21. Strain versus Total Deformation of one Half of the Pipe

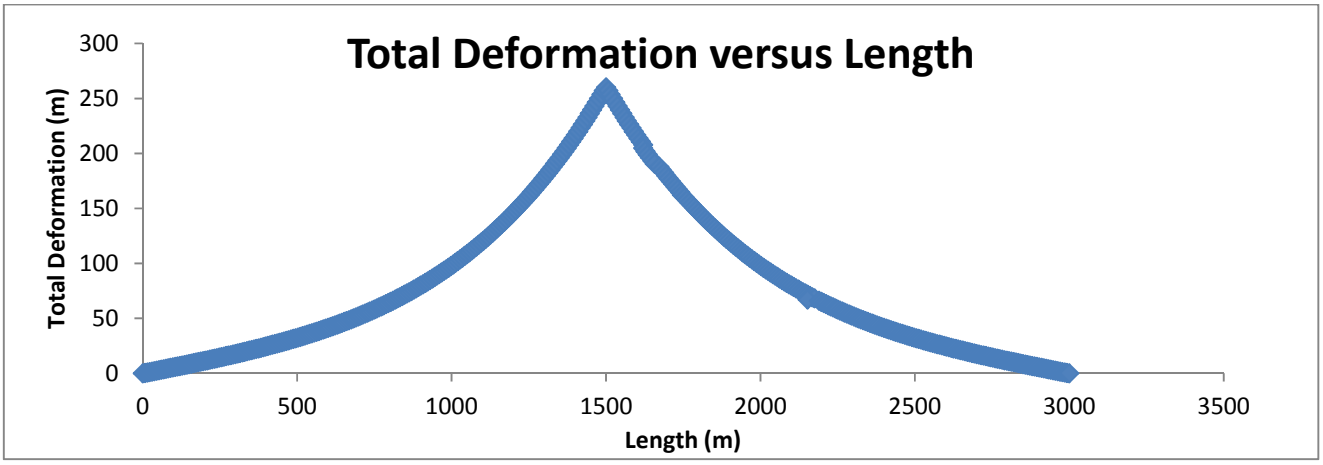

Figure 22. Total Deformation versus Length

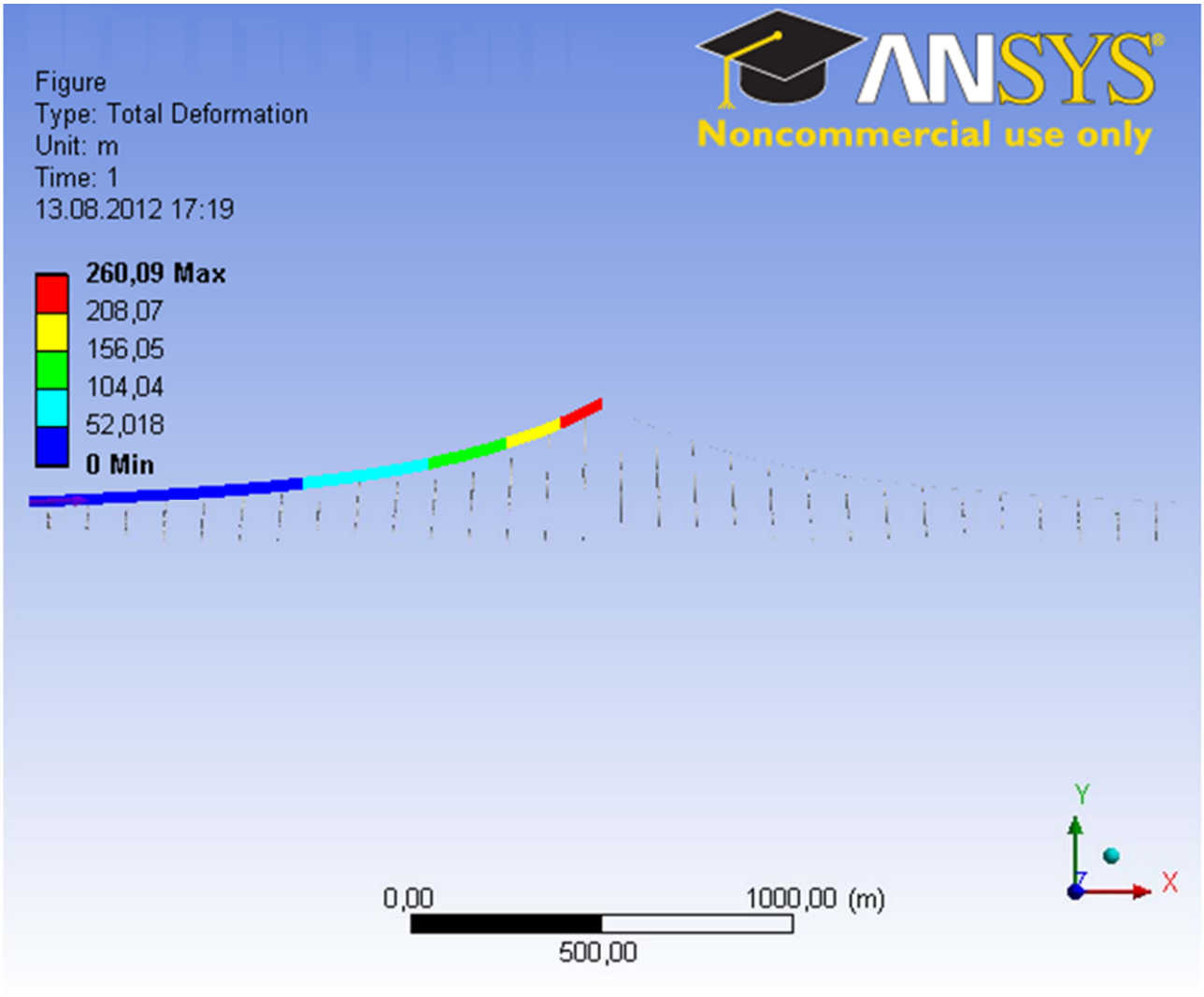

Figure 23. 3-D view of Total Deformation versus Length

The maximum deformation that occurs at the middle of the pipe is almost $260\ m$. *Figure 24* shows the elongation of the pipe's cross-section at the middle of the model (hooking point). The red line in the *Figure 24* is the created path in order to gather the required numerical data.

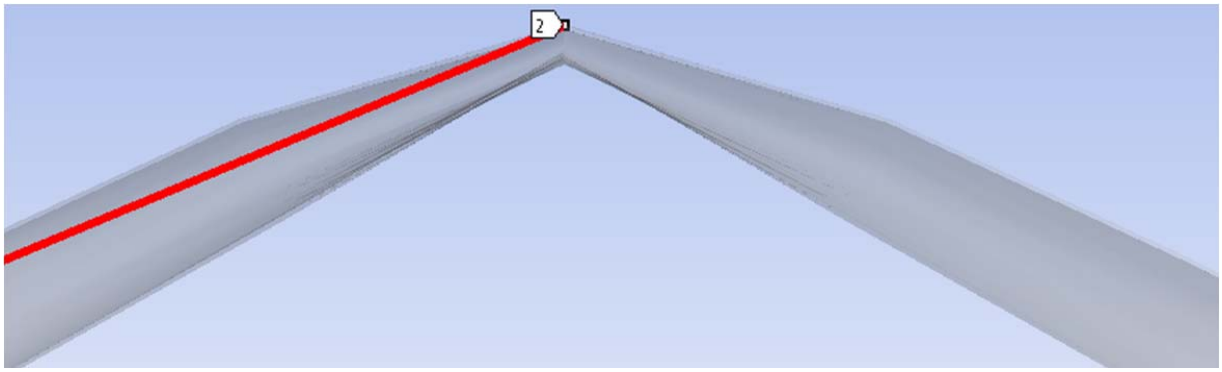

Figure 24. Elongation of the Pipe's Cross-Section at the Hooking Point

6.5 Finite Element model and results – after Rupture

The second step of the finite element analysis represents the post rupture condition. This case was modelled based on the result of the first part. The curved configuration of the pipeline post rupture was determined from the result of the first model. In order to model the curved geometry of the pipeline with respect to the result of the first model, it was decided to choose only some specified cross-sections along the pipeline. The location of the selected cross-sections and related total deformation are presented by *Table 14*.

Table 14. Location and Total Deformation of selected Cross-Section

Location of Selected Cross-Section (m)	Total Deformation (m)	Location of Selected Cross-Section (m)	Total Deformation (m)
60	3,24	840	70,35
120	6,65	900	79,77
180	10,15	960	90,23
240	13,77	1020	102,05
300	17,59	1080	115,22
360	21,63	1140	129,92
420	25,96	1200	146,34
480	30,65	1260	164,34
540	35,75	1320	185,08
600	41,34	1380	207,78
660	47,51	1440	232,92
720	54,33	1500	260,09
780	61,92		

It was assumed that all the boundary conditions at the left and right side of the ruptured cross-section are exactly similar to each other. The symmetry boundary condition was used. Accordingly, this assumption was utilized only for one half of the pipe.

The layers of concrete and anti-corrosion were neglected in this model same as the first model. It should be noticed that the effects of these layers were considered in order to evaluate the applied resisting forces on the pipe.

Subsequently the thrust force was applied from the escaping gas jet at the ruptured pipe's cross-section. One fixed support was applied at the beginning cross-section of the pipe. Outside and inside pressures were applied. The outside pressure is constant and the inside pressure is estimated over time by OLGA which is presented in *Appendix B*.

The used mesh settings were similar to the first model (see *Tables 9, 10, 11* and *12*). Since the length of the post rupture model was one half of the previous model, the created mesh elements and nodes were less. 18540 nodes and 12320 mesh elements were fabricated. *Figure 25* shows a 3-D view of the meshed model after rupture.

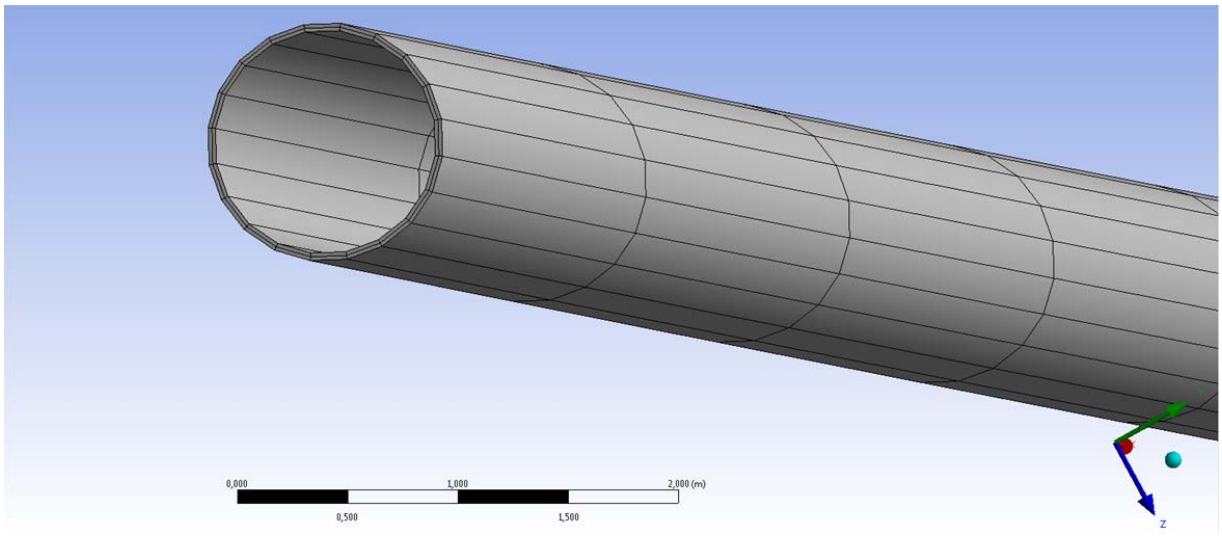

Figure 25. A sample 3-D view of the meshed model after Rupture

A similar method was used in order to apply the resisting forces to the pipeline. Magnitude of the resisting forces were not changed. Twenty nine springs were used but it should be noticed that in order to increase the accuracy more springs were placed at end of the pipeline. It was expected to have less total deformation compared to the first model, thus the APDL commands to make a linear spring to a non- linear spring were written for less deformation with more accuracy. Therefore instead of decreasing the stiffness of the springs for each *10 m* elongation, the stiffness was decreased each $1\ m$ elongation. The place and covered area of the springs are presented by *Table 15*.

Table 15. Location and Covered Area of the Used Springs in the Post Rupture Model

Number of Spring	Location of Spring (m)	Covered Area (m)	Number of Spring (m)	Location of Spring (m)	Covered Area (m)
1	52,5	105	16	1312,5	15
2	157,5	105	17	1327,5	15
3	262,5	105	18	1342,5	15
4	367,5	105	19	1357,5	15
5	472,5	105	20	1372,5	15
6	577,5	105	21	1387,5	15
7	682,5	105	22	1402,5	15
8	787,5	105	23	1417,5	15
9	892,5	105	24	1432,5	15
10	997,5	105	25	1447,5	15
11	1102,5	105	26	1462,5	15
12	1207,5	105	27	1477,5	15
13	1267,5	15	28	1488,5	7,5
14	1282,5	15	29	1496,25	7,5
15	1297,5	15			

As covered areas by springs are not even for all the springs the used APDL commands are not the same for all springs. Similar APDL commands for springs with even covered area were used. The APDL commands as well as the related stiffness of each elongation of springs are presented in *Appendix D*.

One should notice that the used element type for *3-D* modelling of the solid structure in the final step was chosen the same as in the previous step.

Figure 26 displays the 3-D model after rupture just before running the ANSYS.

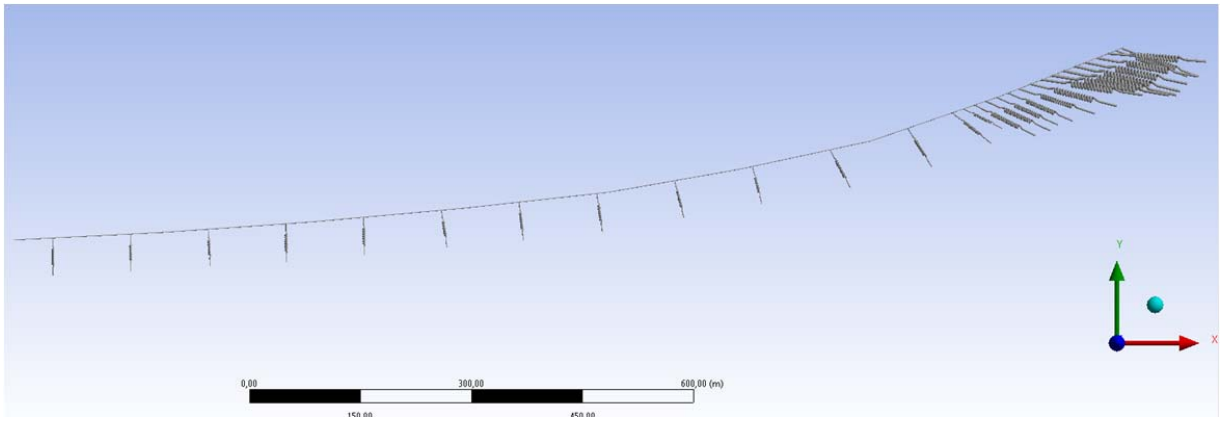

Figure 26. 3-D Model of the Pipe after Rupture just before running the ANSYS

As it was explained more springs were used at the end of the model in order to increase accuracy of the analysis.

Directional deformation and equivalent elastic strain along the pipe were obtained after running the ANSYS.

Table 16 represents initial location, directional deformation and strain of some selected points along the pipe after rupture.

Table 16. Initial Location, Directional Deformation and the Strain of the Pipe Post Rupture

Initial Location (m)		Final Location (m)		Strain (%)	Initial Location (m)		Final Location (m)		Strain (%)	Initial Location (m)		Final Location (m)		Strain (%)
X	*Y*	*X'*	*Y'*		*X*	*Y*	*X'*	*Y'*		*X*	*Y*	*X'*	*Y'*	
0,0000	0,0000	0,000	0,000	0,005	1132,3	127,3	2,28	-18,6	0,390	1272,1	167,0	-2,00	-7,62	0,120
54,690	2,9000	-0,01	-0,94	0,186	1133,1	128,0	2,32	-18,8	0,399	1282,1	172	-1,720	-8,401	0,120
158,91	9,0000	-0,10	-1,63	0,186	1134	128,5	2,36	-19,0	0,410	1290,3	174,6	-1,360	-9,418	0,126
263,13	15,200	-0,22	-1,51	0,182	1137	128,9	2,51	-19,7	0,480	1320,3	185,3	-0,010	-13,18	0,178
367,27	22,100	-0,34	-1,51	0,183	1138	129,4	2,55	-19,9	0,490	1339	191,5	0,950	-15,89	0,228
471,34	29,800	-0,45	-1,53	0,181	1138,8	129,8	2,58	-20,1	0,503	1343,4	194	1,130	-16,39	0,229
575,31	39,000	-0,57	-1,52	0,184	1140,3	130,0	2,64	-21,2	0,530	1351,2	196,8	1,530	-17,50	0,235
684,12	50,000	-0,69	-1,48	0,160	1143,6	131,2	2,76	-21,4	0,580	1371,2	197,8	2,110	-19,17	0,350
788,00	63,000	-0,18	-6,56	0,180	1148,5	131,8	2,88	-21,6	6,53	1379,2	206,8	2,220	-19,56	0,387
890,77	78,000	-0,71	-5,17	0,160	1150	132,5	2,91	-21,8	0,690	1404,2	217,4	1,740	-18,57	0,484
998,00	98,000	-1,42	-1,81	0,170	1153,3	133,0	2,95	-22,1	0,760	1416,5	222,9	0,770	-16,30	0,532
1051,5	108,80	-1,35	-2,21	0,120	1157,9	134,0	2,95	-22,2	0,830	1441	233	-2,225	-9,114	0,591
1061,2	110,50	-1,18	-2,99	0,140	1160,5	134,8	2,91	-22,1	0,790	1448,9	237	-3,963	-4,936	0,596
1106,3	121,00	0,69	-11,4	0,130	1165,5	136,0	2,77	-21,8	0,690	1456,4	240	-5,480	-1,276	0,575
1107,7	121,40	0,78	-11,8	0,130	1173	138,0	2,44	-21,0	0,054	1463,9	243,5	-7,148	2,7637	0,544
1109,3	121,80	0,87	-12,2	0,140	1179,5	140,0	1,97	-19,6	0,409	1472	246,9	-9,003	9,0335	0,251
1110,7	122,40	0,96	-12,6	0,150	1184,5	141,5	1,61	-18,6	0,336	1483	251	-12,47	15,449	0,444
1112,2	122,70	1,13	-13,4	0,170	1192	144,0	1,03	-16,9	0,234	1486	253,9	-13,95	18,976	0,393
1113,7	123,00	1,22	-13,8	0,180	1207	148,5	-0,14	-13,4	0,119	1488,5	255,8	-14,71	20,792	0,362
1115,2	123,50	1,30	-14,2	0,190	1210,1	149,0	-0,51	-12,3	0,119	1491	256,8	-15,47	22,607	0,332
1116,7	124,00	1,39	-14,6	0,210	1230,1	155,0	-1,68	-8,77	0,179	1495,1	257,9	-17,00	26,321	0,253
1118,2	124,40	1,47	-14,9	0,220	1238,5	158,0	-2,03	-7,68	0,192	1497	259	-17,79	28,194	0,231
1119,7	125,00	1,56	-15,3	0,240	1258,5	163,5	-2,23	-7,01	0,154	1500	260,1	-18,57	30,066	0,210
1129,0	126,40	2,12	-14,9	0,350	1262,1	164,9	-2,19	-7,12	0,133					

Figure 27 shows the equivalent elastic-strain along the pipeline. While

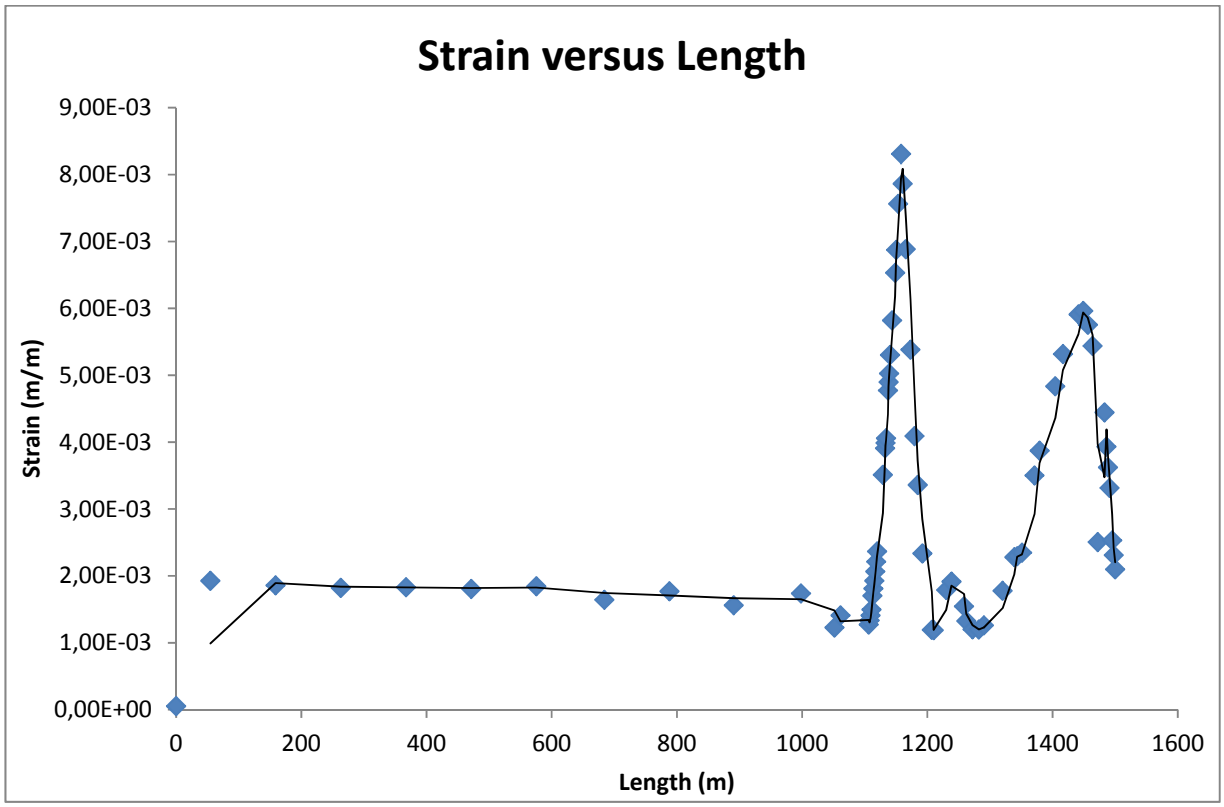

Figure 27. Strain versus Length for after Rupture

Directional deformation is the deformation of pipe in *X* and *Y* direction with respect to the initial location of the pipeline after the rupture; while this initial location is the final location of the pipe just before rupture occurrence. Thus in order to determine the final location of the pipeline it is necessary to sum the initial and final location of the pipeline after the rupture.

Table 17 presents the final location of the pipeline with respect to the pipeline prior to being pulled by the anchor.

Table 17. Final Location of the Pipeline

Initial Location (m)		Final Location (m)		Initial Location (m)		Final Location (m)		Initial Location (m)		Final Location (m)	
X	Y	X''	Y''	X	Y	X''	Y''	X	Y	X''	Y''
0,0000	0,000	0,00000	0,0000	1132,3	0,000	1134,58	108,65	1272,1	0,000	1270,10	159,38
54,690	0,000	54,6800	1,9600	1133,1	0,000	1135,42	109,16	1282,1	0,000	1280,38	163,59
158,91	0,000	158,810	7,3700	1134	0,000	1136,32	109,48	1290,3	0,000	1288,94	165,18
263,13	0,000	282,910	13,690	1137	0,000	1139,51	109,18	1320,3	0,000	1320,24	172,12
367,27	0,000	366,930	20,570	1138	0,000	1140,55	109,51	1339	0,000	1339,95	175,61
471,34	0,000	470,870	28,270	1138,8	0,000	1141,38	109,73	1343,4	0,000	1344,53	177,61
575,31	0,000	574,740	37,480	1140,3	0,000	1142,89	108,83	1351,2	0,000	1352,73	179,30
684,12	0,000	683,430	48,520	1143,6	0,000	1146,32	109,80	1371,2	0,000	1373,31	178,87
788,00	0,000	787,820	56,440	1148,5	0,000	1151,40	110,18	1379,2	0,000	1381,42	187,24
890,77	0,000	890,060	72,830	1150	0,000	1152,91	110,73	1404,2	0,000	1405,94	198,83
998,00	0,000	996,580	96,190	1153,3	0,000	1156,25	110,94	1416,5	0,000	1417,27	206,59
1051,5	0,000	1050,15	106,59	1157,9	0,000	1160,85	111,79	1441	0,000	1439,23	223,89
1061,2	0,000	1060,02	107,50	1160,5	0,000	1163,41	112,67	1448,9	0,000	1444,94	232,06
1106,3	0,000	1106,98	109,61	1165,5	0,000	1168,27	114,16	1456,4	0,000	1450,91	238,72
1107,7	0,000	1108,48	10962	1173	0,000	1175,44	117,04	1463,9	0,000	1456,73	246,26
1109,3	0,000	1110,17	10963	1179,5	0,000	1181,47	120,34	1472	0,000	1463,00	255,93
1110,7	0,000	1111,66	109,84	1184,5	0,000	1186,11	122,92	1483	0,000	1470,53	266,45
1112,2	0,000	1113,37	109,34	1192	0,000	1193,03	127,11	1486	0,000	1472,05	272,88
1113,7	0,000	1114,92	109,25	1207	0,000	1206,86	135,10	1488,5	0,000	1473,79	276,59
1115,2	0,000	1116,52	109,34	1210,1	0,000	1209,59	136,70	1491	0,000	1475,53	279,41
1116,7	0,000	1118,09	109,45	1230,1	0,000	1228,39	146,23	1495,1	0,000	1478,10	284,22
1118,2	0,000	1119,67	109,45	1238,5	0,000	1236,47	150,32	1497	0,000	1479,81	287,19
1119,7	0,000	1121,23	109,67	1258,5	0,000	1256,24	156,49	1500	0,000	1481,43	290,16
1129,0	0,000	1131,12	108,52	1262,1	0,000	1259,91	157,78				

Since the final location of the pipeline is defined a figure can be drawn to show the motion of the pipeline due to the force made by the released gas jet. *Figure 28* shows the pipeline location after rupture due to the hooking force by blue colour; while it uses red colour to illustrate the final location of the pipeline.

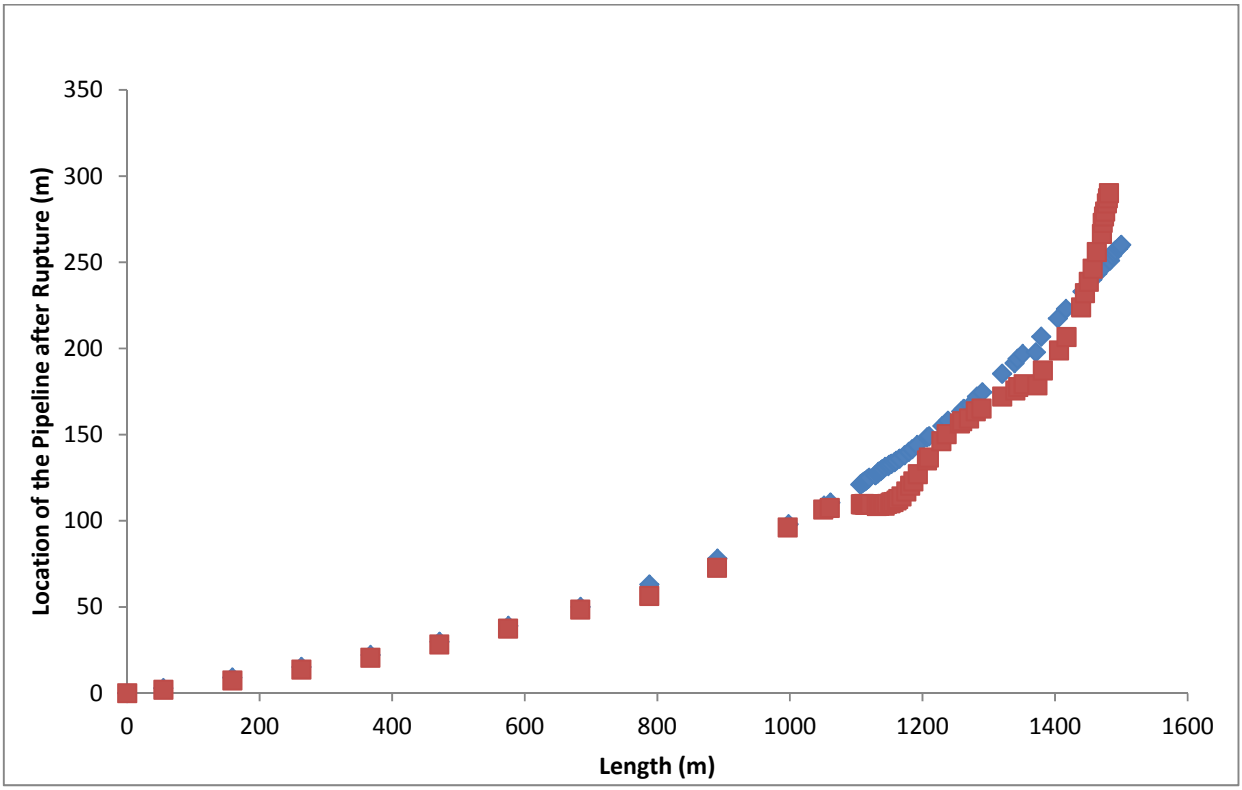

Figure 28. Motion of the Pipeline due to the rupture incident

Figure 29 shows the 3-D model of the pipeline after running the ANSYS.

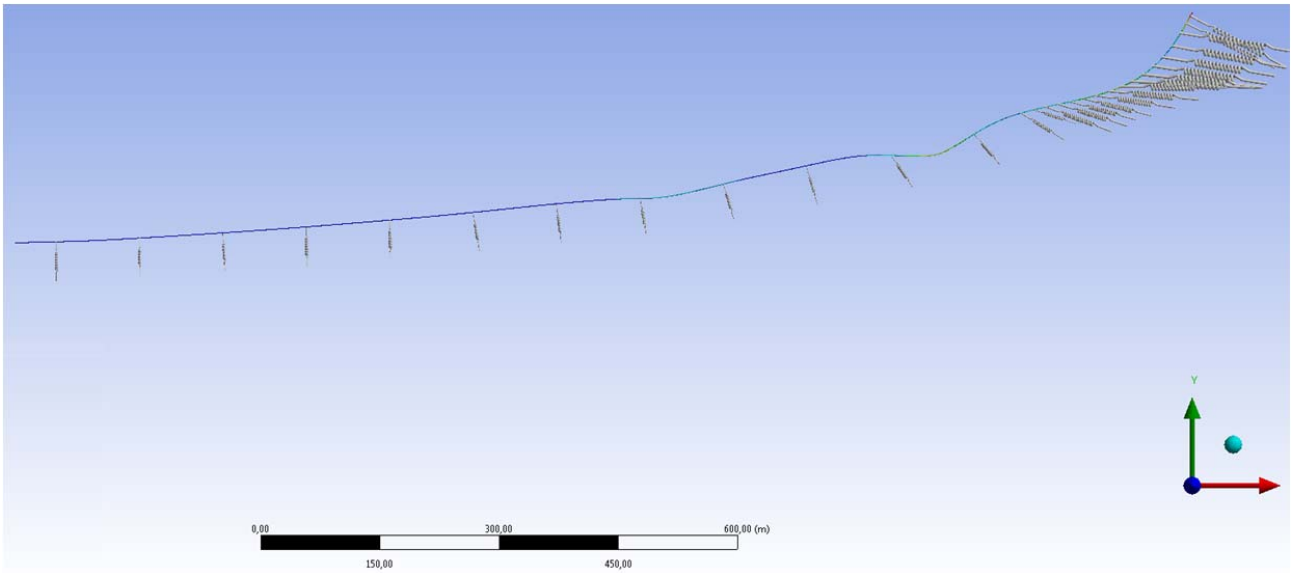

Figure 29. 3-D Model of the Pipeline after running the ANSYS

6.6 Identify Damaged Length

As it was explained before, the pipeline will collapse due to the local buckling. It occurs where strain of entire cross-section reaches $0{,}5\%$. In this study case with respect to the

Table 16 as shown in *Figure 28* two local buckles occur. The first local buckling occurs at $1456m$ and the second one happens at $1157\ m$. In both of them the strain of the entire cross-section is more than $0{,}5\%$. Thus in order to repair the damaged pipeline, the pipe must be cut from the second local buckling region. From the obtained results the furthest cross-section with strain more than $0{,}5\%$ is between $1138\ m$ and$1138{,}8\ m$. Thus $362\ m$ of pipe must be replaced since length of the studied pipe after rupture was $1500\ m$. It should be noted that in the second part of the finite element analysis only one half of the pipe was modelled and it was assumed to have same conditions for the other half. Thus $362\ m$ of the second half will also need replacement.

Hence according to all the boundary conditions as well as made assumptions, the incident destroys $724\ m$ of the pipeline. This length must be removed and replaced in order to repair the submarine pipeline system.

7 Discussion

The Analysis using OLGA identified the pipe's section which generates the largest thrust force from a full bore rupture. Additionally, the analysis determines the fluid condition pre and post rupture. The obtained results and additional hand calculations determine that:

Worst case occurs at	: $KP090$
Internal pressure before rupture is	: $21{,}04\ MPa$
Inside pressure after rupture is	: $20{,}34\ MPa$
Outside pressure is	: $1{,}61\ MPa$
Inside temperature before rupture is	: $9{,}13\ ℃$
Inside temperature after rupture is	: $7{,}27\ ℃$
Maximum mass flow rate is	: $35895{,}11\ kg/m^3$
Maximum pushing force is	: $13{,}38\ MN$

The first step of analysis using ANSYS was based on the flow conditions and assumptions before rupture. The length of the finite element model was $3000\ m$. Results of this analysis determined that the maximum displacement of the pipeline before rupture is almost $260\ m$.

According to the obtained results from OLGA and ANSYS in previous steps, one half of the pipeline was modelled in ANSYS in order to study the response of the pipeline after rupture. Results of this analysis identified that the thrust force due to escaping gas jet caused pipeline to buckle at two regions ($1456m$ and $1157\ m$).

Based on the theory, for local buckling and collapse criteria, and the obtained results of the second finite element analysis the total damaged length can be identified. The total destroyed length of the pipeline due to the incident is approximately $724\ m$.

With OLGA the flow conditions inside the pipeline was determined pre and post rupture. The mass flow rate out of the full bore rupture was calculated and from this, the interaction between fluid and the pipeline was determined. The obtained results show that the released mass flux is high at the rupture moment. This is the consequence of the high pressure and large inventory of the subsea pipeline system. It should be noticed that the assumed diameter of the pipeline is large; therefore a lot of energy is stored in the fluid inside the pipeline.

In the study the equivalent elastic strain at rupture moment was determined. The result showed that if an anchor hooks an offshore pipeline and ruptures the pipeline, displacement of the pipeline before rupturing can be large. The displacement mostly depends on the interaction between seabed and the pipeline, the size of the pipeline, the material properties of the steel pipeline and the hooking load.

It is noteworthy to notice parameters which can postpone the rupture. Firstly, in this study it was assumed that the length of the pipeline will not increase while it is pulled; while in reality the length of

the pipeline increases and a long length of the pipeline (more than $3000\,m$) might be involved. Increasing length of the pipeline postpones the pipe's cross-section at the hooking point to achieve the limit strain for being ruptured. Other terms are related to the ANSYS model. The coating layers were not considered in the finite analysis. These coating layers specially the concrete layer absorb some of the stresses and influence on the rupturing event. Also the interaction between pipeline and the seabed could be modelled more accurate by applying more springs.

There are also conditions that can lead the pipeline to be ruptured earlier than expected. The main topics identified in this study are:

- Three dimensional movement of the pipeline
- Effects of the welding cross-sections between pipe sections
- Exact effect of the impact load
- Residual stresses in the pipeline during installation
- Imperfect features of the used material and coating layers
- Corrosion of the steel pipeline

The above topics were not considered in this analysis due to inherent complexity of them. Therefore the rupture may occur with less pipe deflection and it effectively influences the total displacement of the pipeline. In addition, the interaction between the pipeline and the seabed could be modelled more accurate. The accuracy could be increased by using more springs. This specially affects the extremities of the modelled pipe's section. The effect is less initial displacement than what the results showed.
The effects which cause rupture to occur early dominate over the effects of the terms that delay the rupturing event. Hence the rupture is expected to occur quicker than what it was evaluated. Therefore, it may be assumed that the found solution method is conservative.

The second step of the study showed that the pipeline will be endangered of failing due to local buckling after rupture. Either sides of the ruptured cross-section experience two local buckles. The project used specified criteria to check whether the pipeline fails or not at buckled regions. The onset of collapse depends on various features. Key features are magnitude of the pushing force, mechanical properties of the pipeline steel, the displaced shape of the pipeline as well as the interaction between seabed and the pipeline.

In the second finite element analysis also some conditions that prevent the pipeline from failing were neglected or underestimated. The most important one was the concrete layer which was not modelled. The concrete layer would absorb a portion of the pushing force and resist the pipeline to be bent.

Additionally, one should mention parameters which could cause the pipeline to buckle closer to the ruptured pipe's cross-section. Firstly, if it is assumed that in the first finite element analysis the displacement was exaggerated, it could lead the pipeline not to be buckled far enough from the ruptured cross-section. Also, presence of residual stresses from the bending to rupture weaknesses due to corrosion of the steel pipe as well as the effect of welds in the cross-sections between two pipe sections are not considered. These will all weaken the pipeline and lead to the pipeline to buckle and fail more close to the ruptured cross-section. Therefore, the damaged length may be shorter than the resulting length as calculated in this analysis.

8 Challenges

While doing the analysis, challenges were encountered. The main challenges are listed below:

- Previous research mainly considered a pipeline which is subject to local buckling collapse due to combined loads or being pulled by trawl gears. Additionally, the previous studies which could be used for references investigate the case study with LC condition. Therefore the studied case was quite new and the analysis method had to be developed. Since there was no generally accepted consent on when and where the rupture can occur, identifying the proper criteria was one of the main challenges.
- A large number of hours were needed to acquire skill to utilize the ANSYS software. Various alternatives for analysis were tried during the project. Although obtained results of initial models were deemed unreliable, they consumed much time and energy. As an alternative to the final model, a beam model could be used. The main advantage of a beam model is that the seabed can be modelled by creating a plate on bottom of the beam segment. More accurate result can be achieved when *3-D* model is used. The 3-D model used for the analysis is more calculation intensive. The main challenge in this case was related to find a proper method to apply the resisting forces to the pipeline. Different types of forces such as distributed frictional loads and springs with constant stiffness were tried. Obtained results from this were not satisfactory. The final analysis thus modelled the resisting forces by applying spring. Since the default setting of spring introduces the spring with constant stiffness, it was realised that the result would not be accurate as well. Therefore the springs have been made non-linear by using APDL commands. This part was the most important analysis challenge.
- Training and familiarization with OLGA was less complex than the ANSYS but it also took some time to understand the way of using it for the study.

According to the challenges as well as the mentioned limitations in the chapter 1- section 3, some suggestions will be recommended further.

9 Areas of Further Work

Due to the complexity of this project various assumptions were made in order to solve the problem. The mentioned limitations led to the majority assumptions. Thus it is recommended to survey the limitations more carefully. A more comprehensive study will lead to eliminate the uncertainties cause to. Some elements to be considered in further work are listed below:

- Studying the three dimensional motion of the pipeline
- Surveying the study case with regard to the residual stresses
- Surveying the post rupture case for a longer time period
- Inclusion of the coating layers in the model
- Studying a longer modelled pipe section
- Consideration of the corrosion effects on the pipeline
- Taking into account the imperfectly cylindrical tube cross-section of the pipeline after rupture

In addition the problem can be solved by using LC condition. Then obtained result can be compared with DC condition.

10 Conclusion

The project was interesting since it studied the mechanical response of the pipeline in two totally different steps as well as modelling the fluid flow conditions for steady and unsteady state flow before and after rupture.

During the project, the complexity of the dynamic part of the study showed to be greater than expectation at beginning of the work. The complexity of this part led to most of the assumptions. The effect of these assumptions should be addressed in further studies. One should mention that the assumptions may reduce the accuracy of the results.

As it was explained in *Challenges* chapter finding proper criteria as well as a suitable method to apply the boundary conditions in the analysis still made the analysis difficult. The recommended suggestions by the supervisors were useful in order to carry out the project.

Finally, the predicted response of the pipeline to a hocking force and then to a pushing load was realistic (Vitali, 2012). This shows the developed analysis method is a suitable method. It should not be forgotten that the numerical result can be inaccurate and is governed by the assumptions. Although it was tried to achieve the most accurate and conservative results, it cannot be totally avoided within the short time frame of a master thesis with high amount of limitations and assumptions.

11 References

Boresi, A.P. and Schmidt, R.J., 2003. Advanced Mechanics of Materials. 6th ed. John Wiley & Sons.

DNV, 2010a. Offshore Standard DNV-OS-F101, Submarine Pipeline Systems. Norway: Det Norske Veritas.

DNV, 2010b. Recommended Practice DNV-RP-F107, Risk Assessment of Pipeline Protection. Norway: Det Norske Veritas.

DNV, 2010c. Recommended Practice DNV-RP-F109, On-Bottom Stability Design of Submarine Pipelines. Norway: Det Norske Veritas.

DNV, 2011. Recommended Practice DNV-RP-H103, Modelling and Analysis of Marine Operation. Norway: Det Norske Veritas.

Fox, R.W., McDonald, A.T. and Pritchard, P.J., 2004. Introduction to Fluid Mechanics. 6th ed. Wiley & Sons.

Gudmestad, O.T., 2007. Offshore Pipeline Design. Norway: University of Stavanger (UiS), Faculty of Science and Technology.

Haggag, F.M., 1999. Nondestructive Determination of Yield Strength and Stress-Strain Curves of In-Service Transmission Pipelines Using Innovative Stress-Strain Microprobe™ Technology. USA: Tennessee, Advanced Technology Corporation. [pdf] Available at: <http://www.atc-ssm.com/pdf/dotpipe-fr.pdf> [Accessed 14 August 2012].

HSE, 2009. Guidelines for Pipeline Operators on Pipeline Anchor Hazards. Aberdeen: Health and Safety Executive. [pdf] Available at: <http://www.hse.gov.uk/pipelines/pipeline-anchor-hazards.pdf> [Accessed 14 August 2012].

Hjertager, B., 2011. Lectures of Heat Transfer and CFD. Norway: University of Stavanger (UiS), Faculty of Science and Technology.

Karunakaran, D., 2011. Lecture of Pipeline and Risers– Chapter: Pipeline Hydraulics. Norway: University of Stavanger (UiS), Faculty of Science and Technology.

Kenny, S., 2008. Mechanical Design – Pressure Containment - Part 1, ENGI 8673 Subsea Pipeline Engineering –Lecture 08. University of Newfoundland, Faculty of Engineering and Applied Science Memorial, Available at: <http://www.scribd.com/doc/31905232/08-Mechanical-Design-Pressure-Containment-Part1> [Accessed 14 August 2012].

Munson, B.R., Young, D.F. and Okiishi, T.H., 1998. Fundamentals of Fluid Mechanics, 3rd ed. USA: Iowa, Iowa State University.

Hauch S.R. and Bai Y., 2000. Bending Moment Capacity of Pipes. Journal of Offshore Mechanics and Arctic Engineering. Vol. 122/ 243

Hauch, S.R. and Bai, Y. Use of finite element analysis for local buckling design of pipelines. ASME, 17th International Conference on Offshore Mechanics and Arctic Engineering. Lisbon, Portugal. 1998.

Savidge, J.L., 2000. Compressibility of Natural Gas. ISHM (The International School of Hydrocarbon Measurement). [pdf] Available at:

<http://www.google.no/url?sa=t&rct=j&q=savidge%20j.l.%2C%202000.%20compressibility%20of%20natural%20gas&source=web&cd=1&sqi=2&ved=0CEEQFjAA&url=http%3A%2F%2Fhelp.intellisitesuite.com%2FHydrocarbon%2Fpapers%2F1040.pdf&ei=_aYqUPq1I4zY4QS-2oDwBg&usg=AFQjCNFQjotlcpgO6N8zZJNUVcyPpDh3tw> [Accessed 14 August 2012].

Tritton, D.J., 1988. Physical Fluid Dynamics. 2nd ed. New York: Oxford University Press.

Vitali, L., 2012. Discussion on Subsea Pipeline between Saipem Company and Statoil Company. [Conversation] (Personal communication, Norway: Forus, Statoil, 15th May 2012).

12 Appendix A

Below Figures are obtained by OLGA.

Figure 30 shows inside pressure of the pipeline versus the pipeline length before rupture.

Figure 31 shows geometry of pipeline versus length of the pipeline.

Figure 32 shows variation of pressure at the ruptured cross-section over time post rupture.

Figure 33 shows temperature of the pipeline along the pipeline length before rupture.

Figure 34 shows released mass at ruptured cross-section over time post rupture.

Figure 35 shows density of gas at ruptured cross-section over time after rupture.

Figure 36 shows temperature of the gas at ruptured cross-section over time post rupture.

Figure 37 shows pressure of the gas at ruptured cross-section over time after rupture.

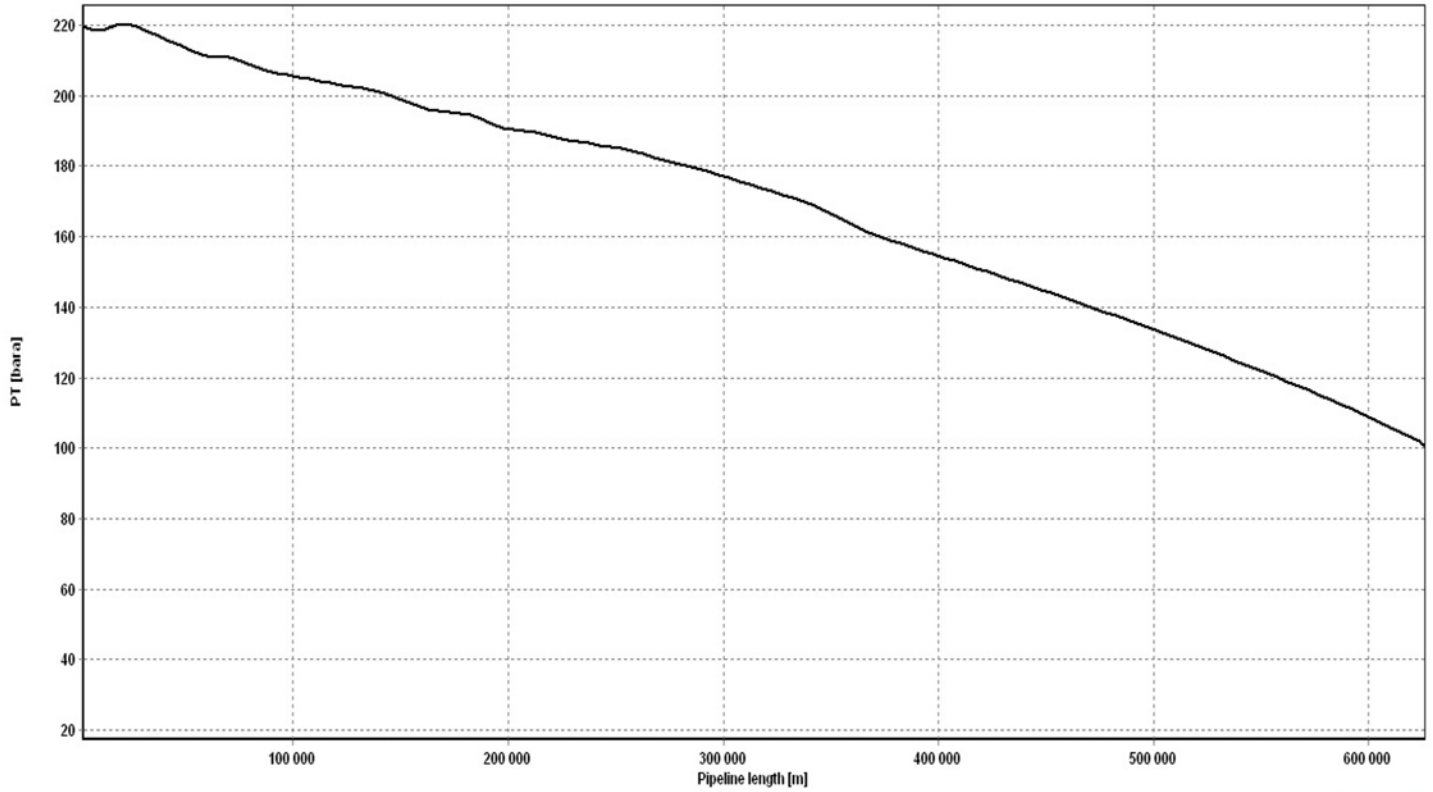

Figure 30. Inside Pressure of the Pipeline versus the Pipeline Length before Rupture

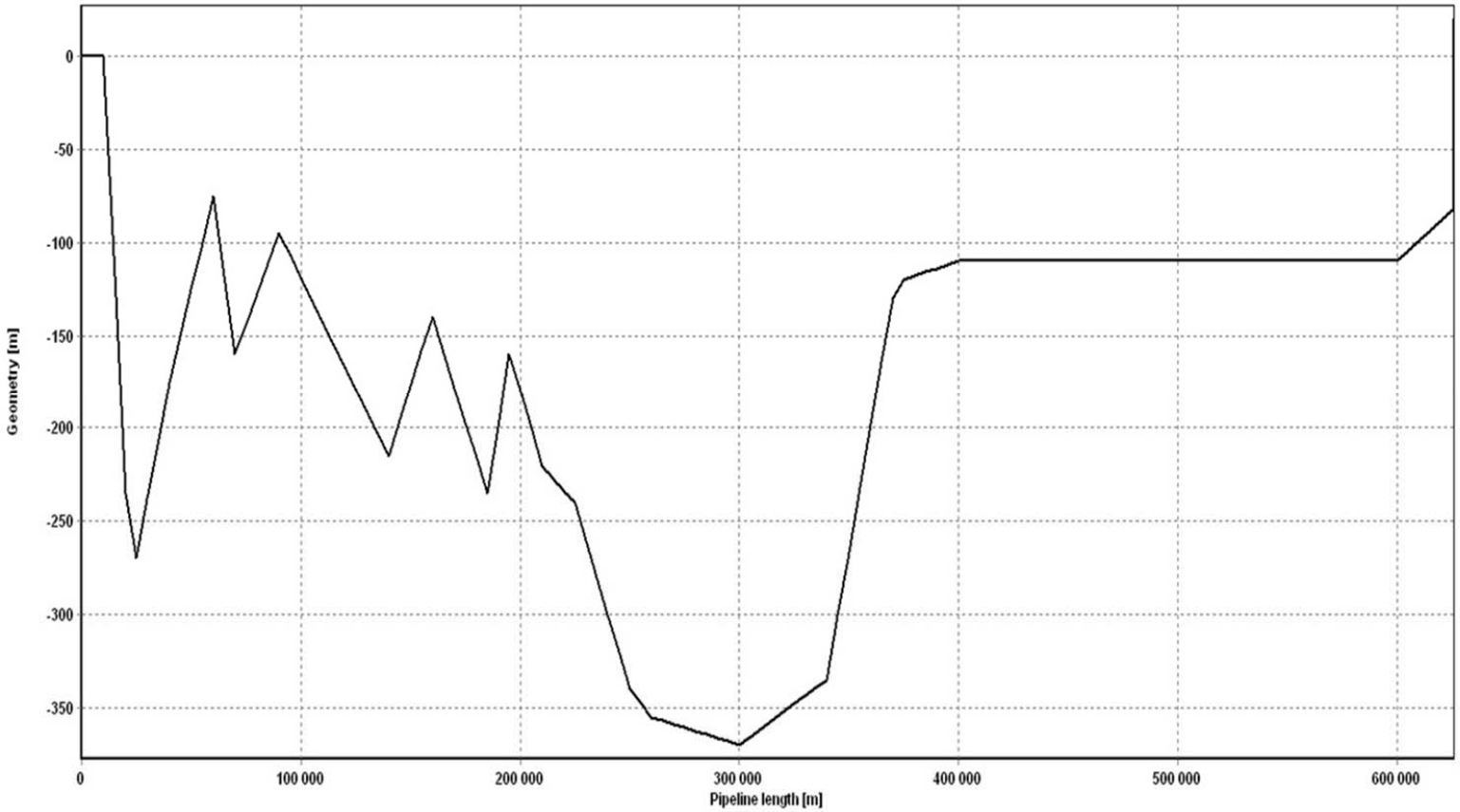

Figure 31. Geometry of Pipeline versus Length of the Pipeline

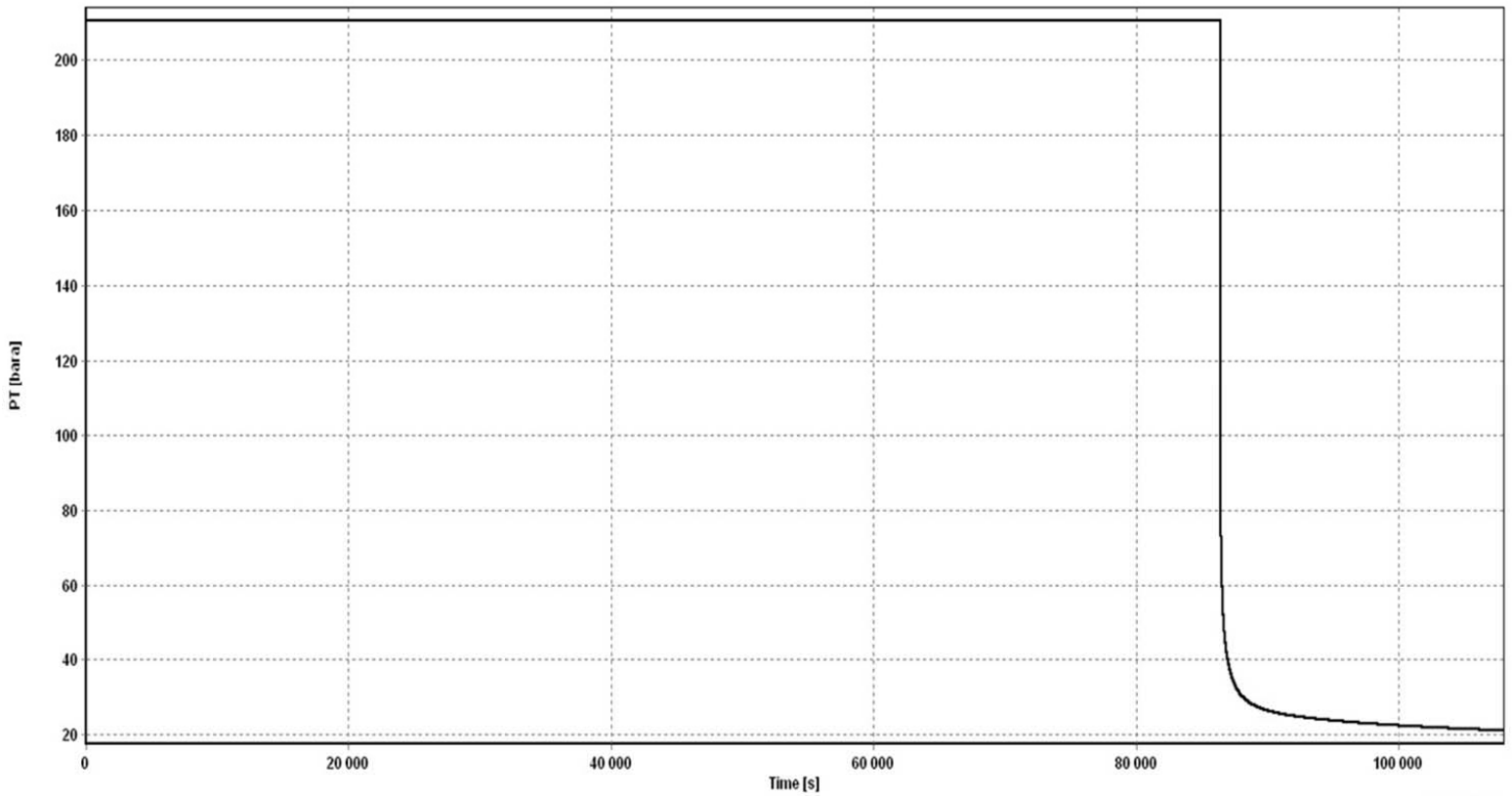

Figure 32. Variation of Pressure at the Ruptured Cross-Section over Time post Rupture

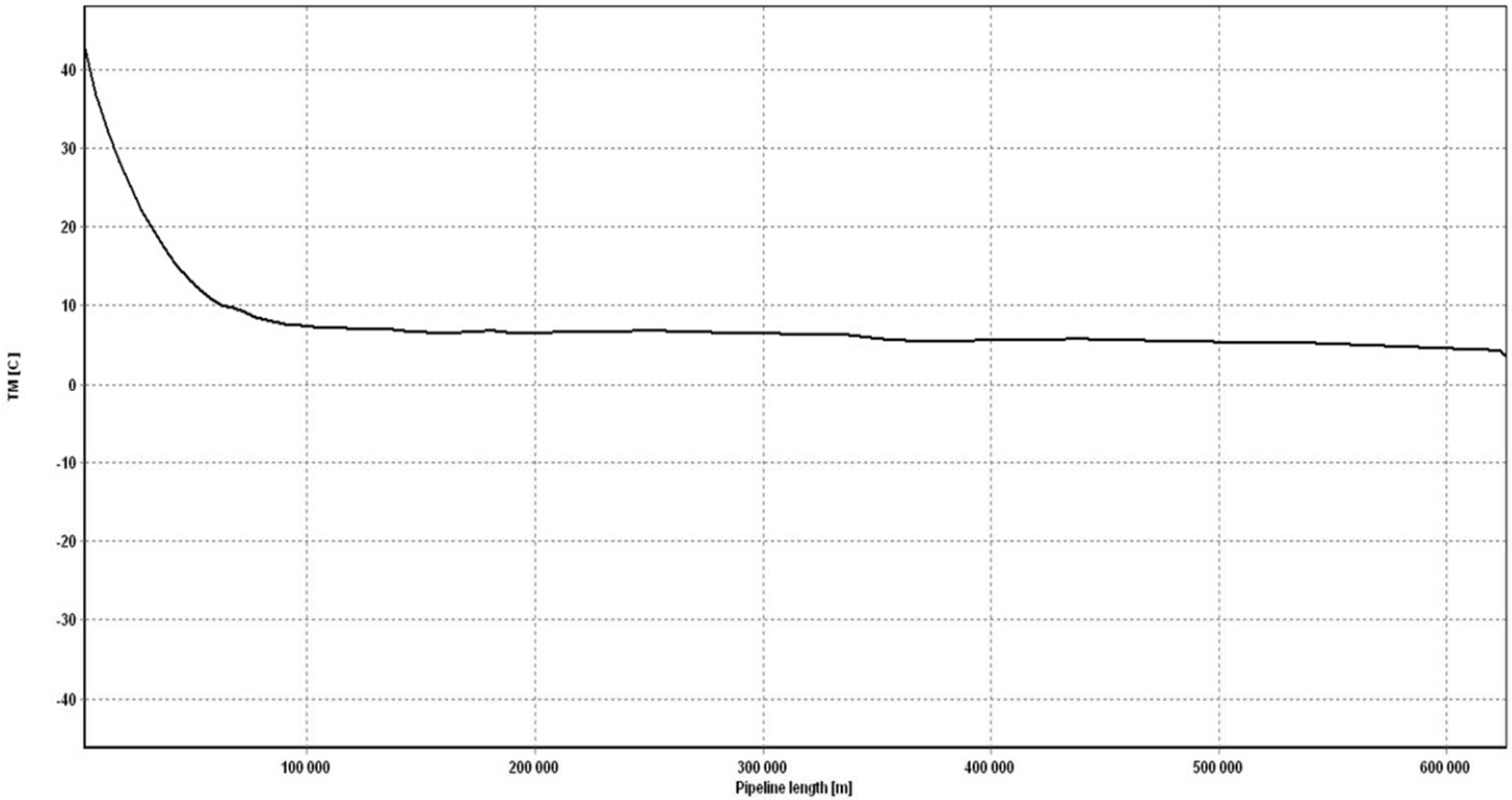

Figure 33. Temperature of Pipeline along the Pipeline Length before Rupture

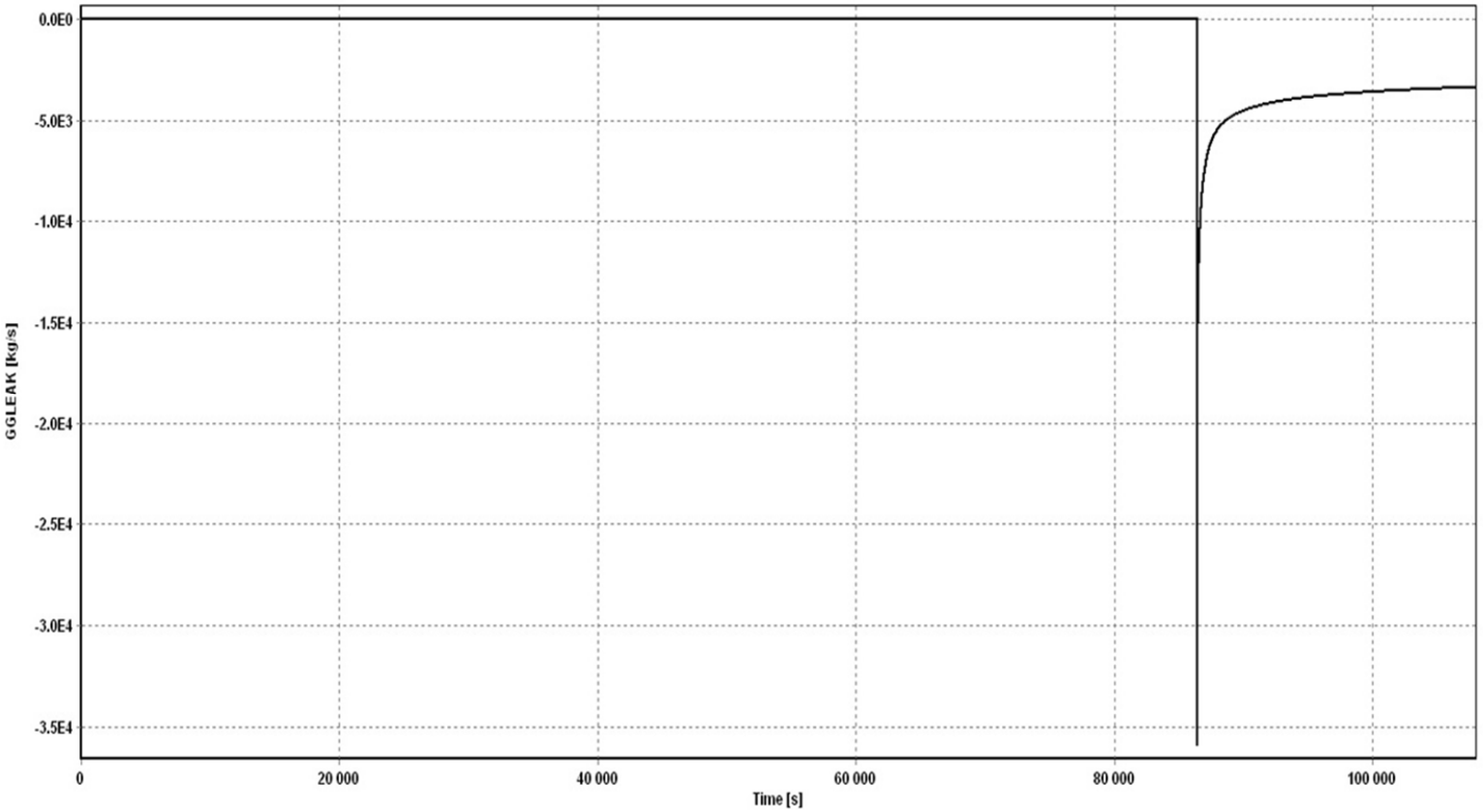

Figure 34. Released Mass at Ruptured Cross-Section over Time post Rupture

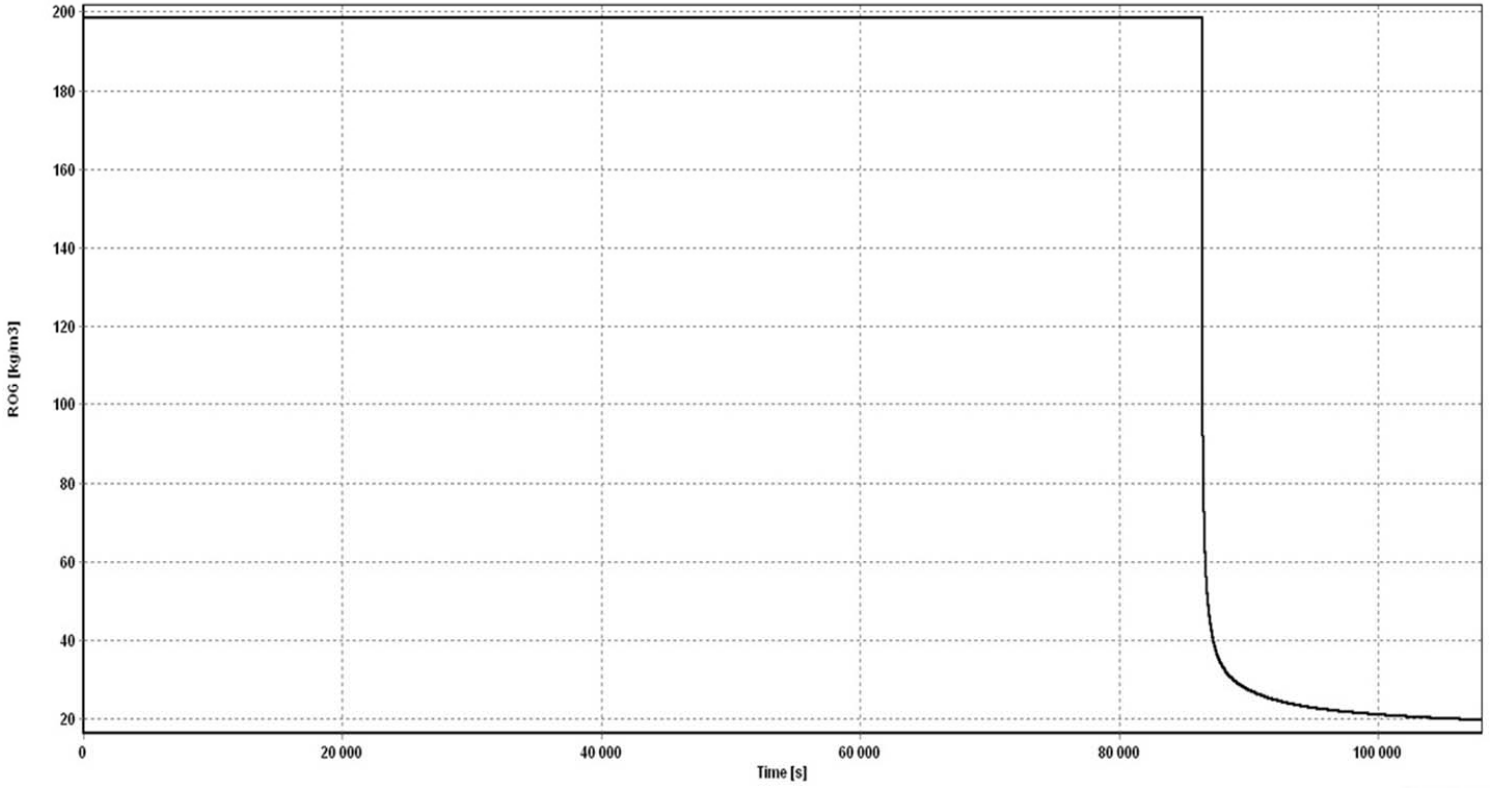

Figure 35. Density of Gas at Ruptured Cross-Section over Time post Rupture

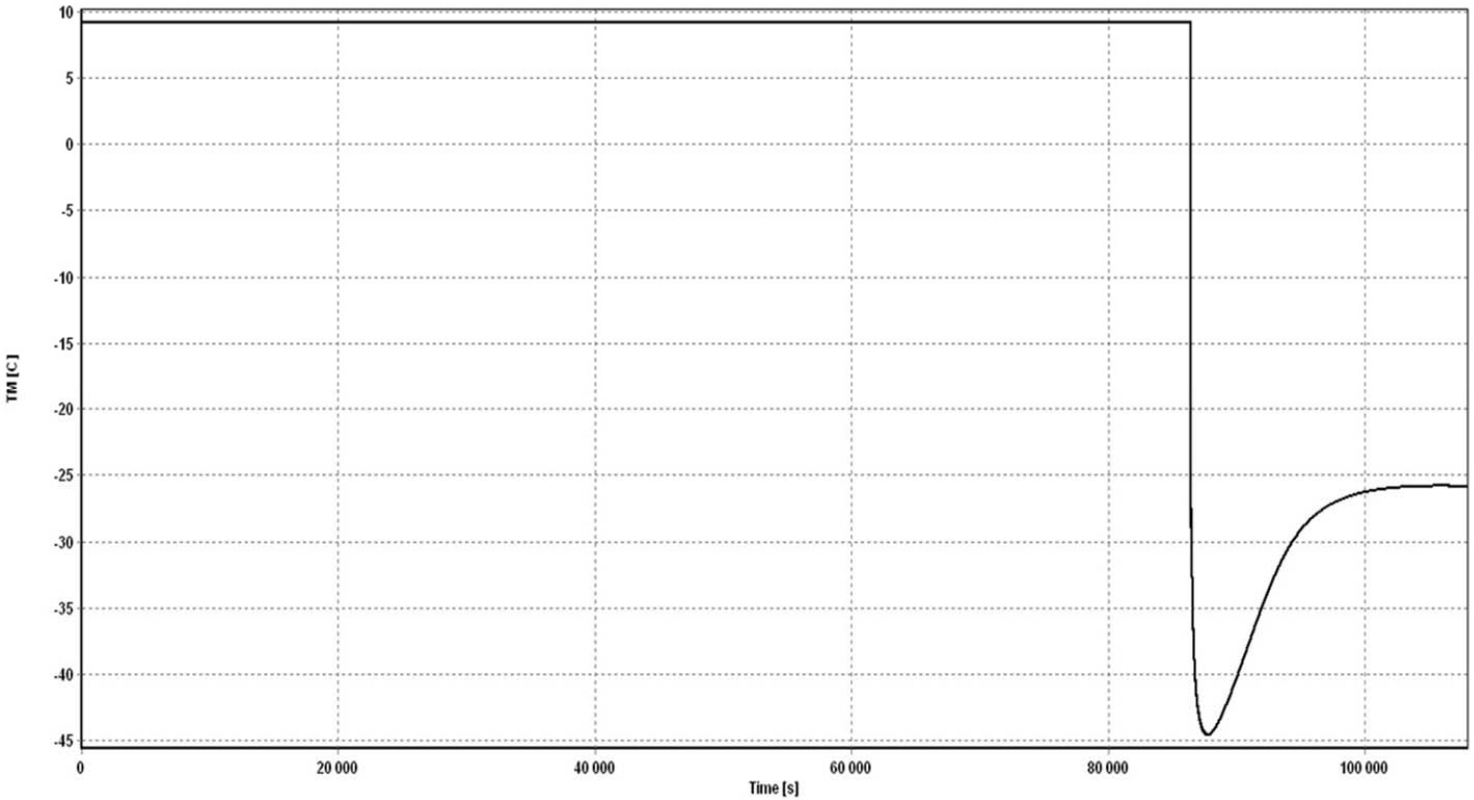

Figure 36. Temperature of the Gas at Ruptured Cross-Section over Time post Rupture

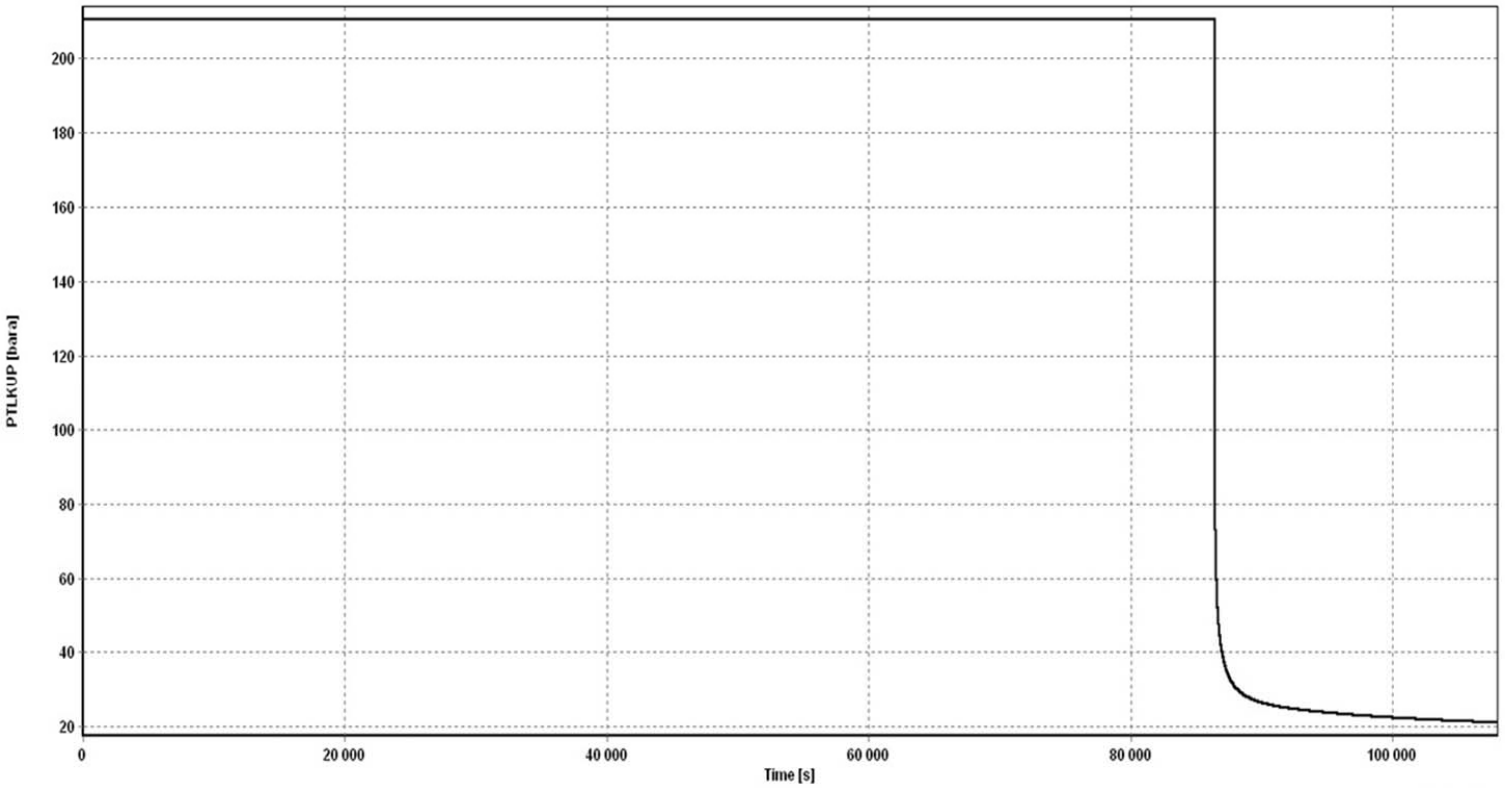

Figure 37. Pressure of the Gas at Ruptured Cross-Section over Time after Rupture

13 Appendix B

Applied force due to release gas can be evaluated based on the mentioned equations in *chapter 3, section 1*. One should notice that due to the transient flow after the rupture density, mass flux and velocity of the fluid depend on time. OLGA only gives the value of the required parameters step by step. Thus the exact functions of the parameters are not accessible and results show that the functions are non-linear. Hence, an assumption was generated in order to linearize the needed functions with high accuracy. In order to increase the accuracy the time step post rupture was chosen small (1,31 sec). Therefore, the assumption which a linear relation exists between each step seems logical. Since the aim is to evaluate the maximum force which it occurs at the rupture moment, only the linearization is done for time interval between rupture instant $(t_0 = 0)$ and the next step $(t_1 = 1{,}31)$. By using this imagination one should only estimate the average value of required parameters between t_0 and t_1. In addition, it is assumed that the flow's direction is normal to the pipe's cross-section and the shape of the cross-section subsequent to rupture is still circular. Hence:

$$P_0 = 210{,}38\ barg$$

$$T_0 = 9{,}13\ ℃$$

$$\bar{\rho} = \frac{\rho_1 + \rho_0}{2} = \frac{183{,}67 + 193{,}55}{2} = 188{,}61\ {}^{kg}/_{m^3}$$

$$A = \frac{\pi}{4} {D_{in}}^2 = \frac{\pi}{4} \cdot 1{,}016^2 = 0{,}811\ m^2$$

$$u_0 = \frac{\dot{m}_0}{A \cdot \rho_0} = \frac{35895{,}11}{0{,}811 \times 193{,}55} = 228{,}68\ {}^{m}/_{s}$$

$$u_1 = \frac{\dot{m}_1}{A \cdot \rho_1} = \frac{32830{,}76}{0{,}811 \times 183{,}67} = 220{,}41\ {}^{m}/_{sec}$$

$$\bar{u} = \frac{u_1 + u_0}{2} = \frac{228{,}68 + 220{,}41}{2} = 224{,}55\ {}^{m}/_{sec}$$

Based on Newton's second law:

$$F = m\frac{du}{dt} + u\frac{dm}{dt}$$

$$\frac{du}{dt} = \frac{u_1 - u_0}{t_1 - t_0} = \frac{220{,}41 - 228{,}68}{1{,}31 - 0} = -6{,}31\ {}^{m}/_{sec^2}$$

$$\frac{dm}{dt} = \bar{\dot{m}} = \frac{\dot{m}_1 + \dot{m}_0}{2} = -34362{,}94\ {}^{kg}/_{sec}$$

If over a short time the V_o is constant:

$$m = \rho V_o \Rightarrow \dot{m} = \dot{\rho} V_o$$

$$\rho_{(t)} = \frac{\rho_1 - \rho_0}{t_1 - t_0} \cdot t + \rho_0 = -7{,}54 \cdot t + 193{,}56$$

$$\dot{\rho} = -7{,}54 \ {}^{kg}/_{m^3 \cdot sec}$$

$$V_o = \frac{\dot{m}|_0}{\dot{\rho}|_0} = \frac{-35895{,}11}{-7{,}54} = 4760{,}6 \ m^3$$

$$m = \bar{\rho} V_o = 188{,}61 \times 4760{,}6 = 897896{,}766 \ kg$$

$$F = 897896{,}766 \times (-6{,}31) + 224{,}55 \times (-34362{,}94) = -13{,}38 \ MN$$

The negative sign expresses the force is compressive force as it was expected.

The inside average pressure and average temperature post rupture are evaluated below:

$$\bar{P} = \frac{P_1 + P_0}{2} = \frac{196{,}60 + 210{,}38}{2} = 203{,}42 \ barg$$

$$\bar{T} = \frac{T_1 + T_0}{2} = \frac{5{,}4 + 9{,}13}{2} = 7{,}27 \ ℃$$

14 Appendix C

First of all it is needed to define whether the mentioned equations are applicable for this project or not. According to the equation (41):

$P_i = 21{,}038\ MPa$ that is more than the $P_e = 1{,}61\ MPa$. In addition, $\frac{D_{out}}{t_2} = \frac{1{,}0842}{0{,}0341} = 31{,}8\ \leq 45$. Thus, the equations are relevant for this special case.

From *Figure 13* and $\frac{D_{out}}{t_2} = \frac{1{,}0842}{0{,}0341} = 31{,}8$ the α_{gw} must be $0{,}9$. In order to compute f_y the α_u as well as $f_{y.temp}$ must be defined while the α_u & $f_{u.temp}$ are required to estimate thef_u. The $\alpha_u$is found from *Table 6* which for normal condition is $0{,}96$. Since the temperature difference is less than 50℃ and with respect to lecture by Shawn Kenny (2008) the $f_{y.temp}$ & $f_{u.temp}$ are equal to $15\ MPa$. Hence:

$$F_y = (450 - 15) \cdot 0{,}96 = 417{,}6\ MPa$$

$$F_u = (535 - 15) \cdot 0{,}96 = 499{,}2\ MPa$$

And then:

$$f_{cb} = Min\left[f_y; \frac{f_u}{1.15}\right] = Min\left[417{,}6; \frac{499{,}2}{1{,}15}\right] = 417{,}6\ MPa$$

$$P_b(t) = \frac{2t}{D_{out} - t} \cdot f_{cb} \cdot \frac{2}{\sqrt{3}} = \frac{2 \cdot 0{,}0341}{1{,}0842 - 0{,}0341} \cdot 417{,}6 \cdot \frac{2}{\sqrt{3}} = 21{,}32\ MPa$$

$$\varepsilon_c(t_2, P_{min} - P_e) = 0{,}78 \cdot \left(\frac{0{,}0341}{1{,}0842} - 0{,}01\right) \cdot \left(1 + 5{,}75 \cdot \frac{21{,}038 - 1{,}61}{21{,}32}\right) \cdot 0{,}93^{-1{,}5} \cdot 0{,}9 = 0{,}105$$

By choosing the low safety class from the *Table 5* which defines the γ_ε (2); the ε_{Rd} will be:

$$\varepsilon_{Rd} = \frac{\varepsilon_c(t_2, P_{min} - P_e)}{\gamma_\varepsilon} = \frac{0{,}105}{2} = 0{,}0525$$

Thus, if the strain due to pull-over exceed $5{,}25$ % the rupture can occur.

15 Appendix D

Soil resistance is made by two parts; first one is called Coulomb Friction and the second one is called passive resistance (F_R) which is due to the penetration of the pipe into the soil. To compute the resisting forces it is necessary to know the total mass of the pipeline as well as the penetration (DNV, 2010c).

- Coulomb Friction load (F_c):
  This friction load is calculated by equation (Gudmestad, 2011):

$$F_c = \mu_f \cdot (N - F_L)$$

  Where μ_f is the coefficient of friction and for a pipe that is covered by a concrete layer is sand is $0{,}6$ (DNV, 2010c); the F_L is vertical (lift) force (Gudmestad, 2011); N is the weight of the submerged pipeline; which is the difference between the weight of the pipe (W) in the air and the buoyancy force (F_B). Calculation of the F_R is represented below (DNV, 2011).

$$W = m_{total} \cdot g$$

  Where m_{total} is the total mass of the pipeline and g is acceleration of gravity that equals to $9{,}81\ m/s^2$. As the incident occurs while the pipeline is in operation to evaluate the mass of the pipeline, it is necessary to consider the mass of contents (fluid) and the absorbed water by the concrete water; as well as the mass of the steel, the concrete layer and the anti-corrosion layer. The density of the fluid was computed by the OLGA model. The total mass of the pipe is estimated by equation:

$$m_{total} = m_{steel} + m_{concrete} + m_{anti-corrosion} + m_{contents} + m_{absorbed\ water}$$

$$m_{steel} = \frac{\pi}{4}\left({D_{out}}^2 - {D_i}^2\right) \cdot \rho_{steel} = \frac{\pi}{4}(1{,}0842^2 - 1{,}016^2) \cdot 7800 = 877{,}64\ {}^{kg}/_{m}$$

$$m_{anti-Corr.} = \frac{\pi}{4}\left({D_{out}}^2 - {D_i}^2\right) \cdot \rho_{anti-Corr.} = \frac{\pi}{4}(1{,}0962^2 - 1{,}0842^2) \cdot 1300 = 26{,}71\ {}^{kg}/_{m}$$

$$m_{concret} = \frac{\pi}{4}\left({D_{out}}^2 - {D_i}^2\right) \cdot \rho_{steel} = \frac{\pi}{4}(1{,}1862^2 - 1{,}0862^2) \cdot 2250 = 363{,}00\ {}^{kg}/_{m}$$

$$m_{contents} = \frac{\pi}{4}{D_i}^2 \cdot \rho_{contents} = \frac{\pi}{4} \cdot 1{,}016^2 \cdot 193{,}55 = 156{,}92\ {}^{kg}/_{m}$$

$$m_{absorbed\ water} = 0{,}04 \cdot m_{concret} = 0{,}04 \cdot 363{,}00 = 14{,}52\ {}^{kg}/_{m}$$

  Hence the total mass is:

$$m_{total} = 877{,}64 + 26{,}71 + 363{,}00 + 156{,}92 + 14{,}52 = \ 1438{,}79\ {}^{kg}/_{m}$$

Thus:

$$W = m_{total} \cdot g = 1438{,}79 \cdot 9{,}81 = 14114{,}53\ {}^{N}/_{m}$$

The lift force depends on the lift coefficient (C_L), pipe's outer diameter and current velocity (V_c) and the density of the seawater (Gudmestad, 2011).

$$F_L = \frac{1}{2} \cdot \rho_{water} \cdot D \cdot C_L \cdot |V_c| \cdot V_c$$

If it is assumed that the current is normal to the pipeline and the C_L is 0,3; then:

$$F_L = \frac{1}{2} \cdot 1025 \cdot 1{,}1862 \cdot 0{,}3 \cdot 0{,}1 \cdot 0{,}1 = 1{,}82\ {}^{N}/_{m}$$

Force that acts upwards to a submerged object due to displacing a specified volume of water is called Buoyancy force (F_B). To evaluate this force the below equation is used:

$$F_B = \rho_{water} \cdot g \cdot V_{submerged}$$

Where ρ_{water} is density of seawater and equals to $1025 kg/m^3$; while $V_{submerged}$ is displaced volume of water that is same as the submerged volume. In this case it equals to the volume of the pipeline; since the pipeline is totally submerged:

$$F_B = 1025 \cdot 9{,}81 \cdot \frac{\pi}{4} 1{,}1862^2 = 11112{,}16\ {}^{N}/_{m}$$

Hence:

$$N = W - F_B = 14114{,}53 - 11112{,}16 = 3002{,}37\ {}^{N}/_{m}$$

And:

$$F_c = \mu_f \cdot (N - F_L) = 0{,}6 \cdot (3002{,}37 - 1{,}82) = 1800{,}33\ {}^{N}/_{m}$$

- Passive Resistance (F_R):

  This resistance is not constant while the pipe moves but for the large displacement it can be assumed to be constant. Below equations are used to define the $F_R$that depends on the penetration (Z_P) (DNV, 2010c).

$$\frac{F_R}{N - F_L} = \begin{cases} \left(5{,}0 \cdot K_S - 0{,}15 \cdot {K_S}^2\right) \cdot \left(\frac{Z_P}{D_{out}}\right)^{1{,}25} & if\ K_S \leq 26{,}7 \\ K_S \cdot \left(\frac{Z_P}{D_{out}}\right)^{1{,}25} & if\ K_S > 26{,}7 \end{cases}$$

and K_S is defined by:

$$K_S = \frac{{\gamma_S}' \cdot {D_{out}}^2}{N - F_L} = \frac{12100 \cdot 1{,}1862^2}{3002{,}37 - 1{,}82} = 5{,}67$$

In this project only the initial penetration is taken into account which is estimated by below equation:

$$\frac{Z_P}{D_{out}} = 0{,}037 \cdot {K_S}^{-0{,}67} = 0{,}037 \cdot 5{,}67^{-0{,}67} = 0{,}012$$

and now the F_R can be evaluated and since the $K_S \leq 26{,}7$ the first equation is used:

$$\frac{F_R}{N - F_L} = \left(5{,}0 \cdot K_S - 0{,}15 \cdot {K_S}^2\right) \cdot \left(\frac{Z_P}{D_{out}}\right)^{1{,}25} = (5{,}0 \cdot 5{,}67 - 0{,}15 \cdot 5{,}67^2) \cdot (0{,}012)^{1{,}25}$$
$$= 0{,}093$$

$$\frac{F_R}{N - F_L} = 0{,}093 \Rightarrow F_R = 0{,}093 \cdot (3002{,}37 - 1{,}82) = 279{,}05 \ {}^{N}/_{m}$$

As it was mentioned before, the total resisting forces $\left(F_f\right)$ on the pipeline is the sum of F_c and F_R, hence:

$$F_f = F_c + F_R = 1800{,}33 + 279{,}05 = 2079{,}38 \ {}^{N}/_{m}$$

As it was mentioned that each spring covers 100 m of the pipe, then the initial stiffness of the springs are:

$$K_{sp} = 2079{,}38 \cdot 100 = 207938 \ {}^{N}/_{m}$$

Where the displacement is 1 m the applied resisting forces to a section of the pipe with $100\ m$ length is:

$$F_s = K_{sp} \cdot X_s = 207938 \cdot 1 = 207937\ N$$

Since the aim is to apply constant resisting forces, then the stiffness is reduced every $10\ m$:

$$K_{sp} = \frac{F_s}{X_s} = \frac{2070937}{X_s}$$

With respect to above equation the related stiffness were evaluated for each deformation.

- Before Rupture:
  In this case it was assumed that the deformation will not reach to $400\ m$, thus the stiffness is changed only for elongations less than $400\ m$. Results are represented by *Table 18*.

Table 18. Related Stiffness of Springs According to Their Elongation before Rupture

Elongation (m)	Stiffness (N/m)	Elongation (m)	Stiffness (N/m)	Elongation (m)	Stiffness (N/m)	Elongation (m)	Stiffness (N/m)	Elongation (m)	Stiffness (N/m)
10	207090	90	2310	170	1223	250	832	330	630
20	10395	100	2079	180	1155	260	800	340	612
30	6930	110	1890	190	1094	270	770	350	594
40	5198	120	1733	200	1040	280	743	360	578
50	4158	130	1600	210	990	290	717	370	562
60	3465	140	1485	220	945	300	693	380	547
70	2970	150	1386	230	904	310	671	390	533
80	2599	160	1300	240	866	320	650	400	520

- Post Rupture:

  In this case it was assumed that the total deformation will not be more than $80\ m$, thus the maximum considered elongation of the springs was $80\ m$. As it was explained before, three different APDL commands were used.

  Tables 19, 20 and *21* represent the stiffness of the similar springs according to the elongation of the springs for springs that cover 105 m, 15 m and $7{,}5$ m, respectively.

  The maximum stiffness for different types of springs is evaluated below:

  $105\ m$ Covered Area:

  $$2079 \times 105 = 218925\ {}^{\mathrm{N}}/_{\mathrm{m}}$$

  $15\ m$ Covered Area:

  $$2079 \times 15 = 31185\ {}^{N}/_{m}$$

  $7{,}5\ m$ Covered Area:

  $$2079 \times 7{,}5 = 15592\ {}^{N}/_{m}$$

Table 19. Related Stiffness of Springs with 105 m Cover Area According to Their Elongation after Rupture

Elongation (m)	Stiffness (N/m)	Elongation (m)	Stiffness (N/m)	Elongation (m)	Stiffness (N/m)	Elongation (m)	Stiffness (N/m)	Elongation (m)	Stiffness (N/m)
0	0	17	12841	34	6420	51	4280	68	3210
1	218295	18	12128	35	6237	52	4198	69	3163
2	109147	16	11489	36	6063	53	4118	70	3118
3	72765	20	10915	37	5899	54	4042	71	3074
4	54573	21	10395	38	5744	55	3969	72	3031
5	43659	22	9922	39	5597	56	3898	73	2990
6	36382	23	9491	40	5457	57	3829	74	2949
7	31185	24	9095	41	5324	58	3764	75	2910
8	27286	25	8731	42	5197	59	3699	76	2872
9	24255	26	8396	43	5076	60	3638	77	2835
10	21829	27	8085	44	4961	61	3578	78	2798
11	19845	28	7796	45	4851	62	3520	79	2763
12	18191	29	7527	46	4745	63	3465	80	2728
13	16791	30	7276	47	4644	64	3410		
14	15592	31	7041	48	4547	65	3358		
15	14553	32	6821	49	4455	66	3307		
16	13643	33	6615	50	4365	67	3258		

Table 20. Related Stiffness of Springs with 15 m Cover Area According to Their Elongation after Rupture

Elongation (m)	Stiffness (N/m)	Elongation (m)	Stiffness (N/m)	Elongation (m)	Stiffness (N/m)	Elongation (m)	Stiffness (N/m)	Elongation (m)	Stiffness (N/m)
0	0	17	1834	34	917	51	611	68	458
1	31185	18	1732	35	891	52	599	69	451
2	15593	16	1641	36	866	53	588	70	445
3	10395	20	1559	37	842	54	577	71	439
4	7796	21	1485	38	820	55	567	72	433
5	6237	22	1417	39	799	56	556	73	427
6	5197	23	1356	40	779	57	547	74	421
7	4455	24	1299	41	760	58	537	75	415
8	3898	25	1247	42	742	59	528	76	410
9	3465	26	1199	43	725	60	519	77	405
10	3118	27	1155	44	708	61	511	78	399
11	2835	28	1113	45	693	62	502	79	394
12	2598	29	1075	46	677	63	495	80	389
13	2398	30	1039	47	663	64	487		
14	2227	31	1006	48	649	65	479		
15	2079	32	974	49	636	66	472		
16	1949	33	945	50	623	67	465		

Table 21. Related Stiffness of Springs with 7,5 m Cover Area According to Their Elongation after Rupture

Elongation (m)	Stiffness (N/m)	Elongation (m)	Stiffness (N/m)	Elongation (m)	Stiffness (N/m)	Elongation (m)	Stiffness (N/m)	Elongation (m)	Stiffness (N/m)
0	0	17	917	34	458	51	305	68	229
1	15593	18	866	35	445	52	299	69	225
2	7796	16	820	36	433	53	294	70	222
3	5197	20	779	37	421	54	288	71	219
4	3898	21	742	38	410	55	283	72	216
5	3118	22	708	39	399	56	278	73	213
6	2598	23	677	40	389	57	273	74	210
7	2227	24	649	41	380	58	268	75	207
8	1949	25	623	42	371	59	264	76	205
9	1732	26	599	43	362	60	259	77	202
10	1559	27	577	44	354	61	255	78	199
11	1417	28	556	45	346	62	251	79	197
12	1299	29	537	46	338	63	247	80	194
13	1199	30	519	47	331	64	243		
14	1113	31	502	48	324	65	239		
15	1039	32	487	49	318	66	236		
16	974	33	472	50	311	67	232		

A summary of the used APDL commands for the model prior to rupture is written below. As it was noticed before the same APDL commands were used for the model post rupture and only decreasing rate of the stiffness of the springs was different.

```
Spring=CS_Actuator.Find(_sid)
Spring=CS_Actuator.Find(_sid)
spring_table=System.Array.CreateInstance(float,81,2)
# LENGTH transition values
spring_table[0,0]=10.
spring_table[1,0]=20.
spring_table[2,0]=30.
.
.
.
# Spring Stiffness
spring_table[0,1]=20790.
spring_table[1,1]=10395.
spring_table[2,1]=6930.
.
.
.
stiffness = CS_PointsTable(spring_table)
Spring.SetTable(stiffness)
```